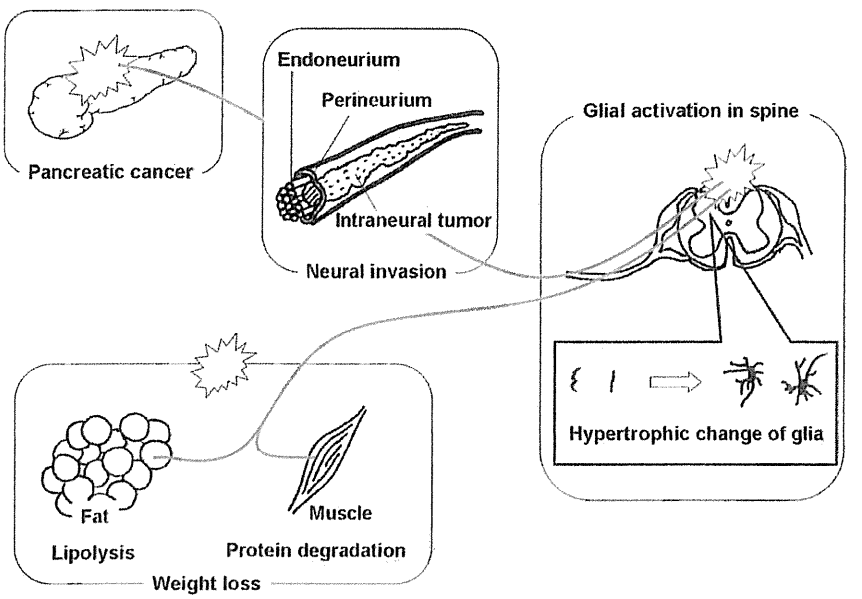


Figure 1. Summarizing scheme of the relationships among N-inv in pancreatic cancer, glial activation in the spinal cord and systemic cachectic changes. N-inv mediates cachectic changes *via* neural routes including spinal cord glia.



states that severe radiological PVST corresponds to a deteriorating systemic condition such as cachexia. Cachexia includes BW loss, loss of muscle and/or fat mass, fatigue, anorexia, anemia, hypoalbuminemia and an elevated circulating level of C-reactive protein (CRP), an inflammatory marker.[20] The correlation between cachectic factors and PVST reinforces the possibility that cachexia is caused by N-inv in pancreatic cancer.

The physiological effects of N-inv can be investigated using animal models. We established a murine model of N-inv by injecting Capan-1 cells, a human pancreatic cancer cell line, into murine sciatic nerves.[21] Intraneural Capan-1 cells form a ductal shape and continuously invade sites proximal to the injected portion of the sciatic nerve, but not peripheral sites.[21] These morphological characteristics of the experimental N-inv tumors mimic human pancreatic cancer. Our N-inv model should therefore be suitable for evaluating the physiological effects of N-inv in pancreatic cancer. Experimental cancer cachexia is defined as BW loss without a reduction in food intake in the presence of a small tumor mass.[22] Because our mouse model meets this definition, the N-inv model is considered a suitable model of experimental cancer cachexia.

The aim of our study was (1) to evaluate the physiological effects of N-inv and (2) to investigate the role of spinal cord glial activation by N-inv in cachexia using clinical data from patients with pancreatic cancer and the N-inv model.

## Material and Methods

### Ethics committee approval

The animal experiments were carried out in accordance with the Guidelines of the Animal Care and Use Committee of the National Cancer Center. The human studies were approved by the National Cancer Center Ethics Committees, and only patients from whom written informed consent was obtained were examined.

### Study protocols of human pancreatic cancer

A validation study of radiological N-inv compared to histological N-inv was performed in four autopsy cases (two women, two men; median age, 71.5 years; range, 67–89; primary tumor sites in the pancreatic head/body and tail, 1/3) in 2006. The pancreas and abdominal aorta with CeA and SMA were resected *en bloc* by one investigator (S.M.). The entire tissue block was sectioned at a right angle to the abdominal aorta at intervals of 5–10 mm. The gross appearance was recorded. The thoracic and lumbar spinal cords were harvested and cut into segments by two investigators (S.M. and A.O.). Radiological N-inv was assessed using CT (SOMATOM definition: Siemens, Munich, Germany or Aquilion: Toshiba, Tokyo, Japan) within 2 months before the autopsy. Images were obtained in the portal phase with a 5-mm slice thickness. The criteria for radiological N-inv on the CT images were (1) PVST around the SMA and the CeA and (2) PVST contiguous with the primary pancreatic tumor. The degree of radiological N-inv was classified as high or low N-inv according to the severity of PVST around the SMA and the CeA. Low radiological N-inv was defined as PVST that encircled neither the SMA nor the CeA completely. The complete encirclement of PVST around the SMA or the CeA was defined as high radiological N-inv. The definition and classification of radiological N-inv were evaluated by comparing the radiological and

histological findings around the SMA and the CeA in the autopsy cases. The CT findings were evaluated by one investigator (A.I.) under the guidance of another investigator (S.M.).

Radiological N-inv and the presence of cachexia were then compared in 50 patients (29 women, 21 men; median age, 66.5 years; range, 44–85; primary tumor sites in the pancreatic head/body/tail, 22/23/5) with pathologically confirmed advanced pancreatic cancer who were treated at National Cancer Center Hospital East, Japan between June 2008 and November 2009. None of the patients had received any previous anticancer treatment and were scheduled to undergo chemotherapy. Patients with liver metastasis were excluded. BW, body mass index (BMI), blood samples and CT images were obtained before initiating chemotherapy. Serum noradrenaline levels were determined with high performance liquid chromatography (HPLC) at SRL, Japan. Patients were assigned to either a high or low N-inv group according to the above definition of radiological N-inv on the CT images.

### Cells

Two human pancreatic cell lines, Capan-1 and BxPC-3, were obtained from the American Type Culture Collection (ATCC). Cancer cells were propagated and subcultured according to the recommended protocol of the ATCC. The cells were used within 2 months after resuscitation of frozen aliquots, and were incubated at 37°C in an atmosphere of 5% $CO_2$ in air. Cancer cells were authenticated on the basis of viability, growth and morphology.

### Mouse model

Male severe combined immunodeficiency (SCID) mice (Clea Japan, Tokyo, Japan; $n = 61$; 9-week-old) were housed in a light- and temperature-controlled room and fed standard food *ad libitum* (irradiated CMF; Oriental Yeast, Tokyo, Japan). According to a previous report,[21] the N-inv model was induced in eight and seven mice using Capan-1 and BxPC-3 cells, respectively. Briefly, $2.5 \times 10^4$ cancer cells were injected into the sciatic nerve. To investigate the effects of sham operation and subcutaneous tumors, the phosphate-buffered saline group (PBS, $n = 4$ each) and the subcutaneous tumor group (SC, $n = 8$, $n = 7$, respectively) were produced by injecting 2.5 μl PBS into the sciatic nerve and by subcutaneous injection of $2.5 \times 10^4$ cancer cells in 100 μl Matrigel (Becton, Dickinson and Company, Franklin Lakes, NJ) into the left flank, respectively. The sciatic nerve was ligated at a site 5 mm proximal to inoculation using a 3-0 silk thread (Alfresa Pharma, Osaka, Japan) in the PBS mice ($n = 4$) and the N-inv mice with Capan-1 cells ($n = 5$). For controls, nonligated PBS mice ($n = 3$) and N-inv mice ($n = 5$) were used. Propentofylline (PPF), a inhibitor of glial activation,[14] at a dose of 10 mg/kg (Sigma, St. Louis, MO) or the saline vehicle ($n = 3$/treatment) was administered to N-inv mice with Capan-1 cells by intraperitoneal (i.p.) injection. Treatment was initiated 3 days before cancer cell injection and was continued daily until the end of the experimental period. Food intake 3 or 4 days per week was measured, and the mean intake per day was recorded.

All mice were deeply anesthetized with i.p. injections of pentobarbital sodium (50 mg/kg) during surgery and were euthanized at 6 weeks after surgery with an overdose of pentobarbital sodium (150 mg/kg, i.p.). After taking blood samples from the posterior vena cava as well as samples of bilateral epididymal fat tissue, bilateral greater pectoral muscle and thoracic/lumbar spinal cord (the 13th thoracic spinal cord [Th13]/the first lumbar spinal cord [L1]), the tumors were harvested and weighed. Serum noradrenaline levels were determined with HPLC (dilution of 1-1/10, SRL).

### Real-time RT-PCR

Quantitative real-time RT-PCR was performed as previously described.[21] The primer sequences are shown in Supporting Information Table 1. The target mRNA level was normalized to the GAPDH level in each sample for standardization. The standardized ratio was converted into fold change of the mean standardized ratio of the experimental control group for normalization, and this normalized level was recorded. In the autopsy cases, the standardized mRNA ratio of Th10 was rated against that of L1 for personalization, and this personalized mRNA level was recorded.

### Histological analysis

The resected specimens obtained from the animals and autopsy tissues were fixed with 4% paraformaldehyde and 10% formaldehyde, embedded in paraffin and cut into serial 3-μm thick sections. The sections were stained with hematoxylin and eosin (HE) and evaluated using light microscopy.

### Quantification of adipocyte size

To quantify adipocyte size, HE-stained sections of fat tissue were analyzed using an ECLIPSE E1000 microscope (Nikon) equipped with a digital camera (DXM1200F, Nikon). The mean size of adipocytes was calculated according to a previous report.[23] Briefly, the number of adipocytes was counted in four random parts per section at a magnification of 100×, and the mean area of adipocytes was calculated.

### Immunohistochemical (IHC) analysis

After deparaffinization, the sciatic nerve sections were immersed in proteinase K (DAKO, Glostrup, Denmark) for 1 min, and incubated with an antibody against human cytokeratin AE1/3 (1/100, DAKO, Glostrup, Denmark) overnight at 4°C. Spinal cord sections (6 μm thick) were treated with microwave heating in 0.01 M citrate buffer or a high pH buffer after deparaffinization. Then, the slides were incubated with an antibody against mouse GFAP (1/2000, Millipore, Billerica, MA), an antibody against human GFAP (1/1000, Dako, Glostrup, Denmark) or an antibody against ionized calcium binding adaptor molecule 1 (Iba-1, 1/1000, Wako, Osaka, Japan) at 4°C overnight. The sections were

incubated in a 0.1% Luxol Fast Blue (LFB) solution at 56°C for 20 hr. The gray matter was divided into four parts (ipsilateral dorsal horn, ipsilateral anterior horn, contralateral dorsal horn and contralateral anterior horn) as shown in Supporting Information Figure 5. The summed areas of GFAP- or Iba1-immuno-positive cell bodies within each area were measured using the Automeasure function of Axio Vision 4.7.1. (Carl Zeiss, Oberkochen, Germany). Then, the positive cell area ratio (summed area of target protein immuno-positive cell bodies/measured area) was calculated. The positive cell area ratios were normalized by converting them into fold change of values of the experimental control groups. Similar to mRNA analysis, L1 was used as an internal control for personalization in the autopsy cases. The mean of the normalized positive cell area ratios in the Th13 ipsilateral dorsal horn or the personalized positive cell area ratios in the Th10 bilateral dorsal horn were recorded.



### Microarray analysis

For microarray analysis, we used GeneChip Mouse 420 2.0 arrays (Affymetrix, Santa Clara, CA, http://www.affymetrix.com). Target cRNA was generated from 100 ng total RNA from each sample using Two-Cycle Target Labeling and Control Reagents (Affymetrix). The procedures for target hybridization, washing and staining with signal amplification were conducted according to the supplier's protocols (http://www.affymetrix.com/support/technical/manual/expression_manual.affx). The arrays were scanned with a GeneChip Scanner 3000 (Affymetrix), and the intensity of each feature of the array was calculated using GeneChip Operating Software v1.1.1 (Affymetrix). The mean intensity was standardized to the target intensity, which was set to 1,000, to reliably compare variable multiple arrays. The values were log transformed and median centered. GeneSpring (Agilent Technologies, Santa Clara, CA, http://www.agilent.com) and Excel (Microsoft, Redmond, WA, http://www.microsoft.com) were used for gene selection. Overexpressed genes (more than twice as high as in PBS) in L1 of N-inv mice (Capan-1) compared to those in the PBS and SC mice were selected. Thirty-five genes are shown in Supporting Information Table 2. All the microarray data have been deposited in a MIAME compliant database, GEO; the accession number SuperSeries GSE34189.

### Statistical analysis

A two-tailed unpaired Student's *t*-test was used to evaluate differences in the various parameters. A $p$ value $<0.05$ was considered significant. Statistical analysis was performed using the Statview-J 5.0 package, Windows version (SAS).

## Results

### N-inv and cachexia in patients with pancreatic cancer

PVST encircling the SMA and the CeA on CT images is regarded clinically as extrapancreatic N-inv.[19] The degrees of N-inv and cachexia were assessed using PVST around the SMA and the CeA on CT images and clinical data from 50 patients with advanced pancreatic cancer. Patients with or without PVST encircling the SMA or CeA were assigned to the low N-inv group (Fig. 2*a*) or the high N-inv group (Fig. 2*b*), respectively. Before chemotherapy, the percentage of patients with high N-inv was 48.0% ($n = 24$). At that time, BW and the BMI were low in the high N-inv patients (mean BW, 51.7 kg, 95% CI, 48.1–55.3, $p = 0.1655$; mean BMI, 20.5 kg/m$^2$, 95% CI, 19.4–21.7, $p = 0.0396$), compared to low N-inv patients (mean BW, 55.3 kg, 95% CI, 51.5–59.2; mean BMI, 22.4 kg/m$^2$, 95% CI, 21.0–23.8) (Fig. 2*c*). The levels of plasma CRP and noradrenaline tended to be high in the high N-inv group (mean CRP, 1.02 mg/dl, 95% CI, 0.21–1.82, $p = 0.1227$; mean noradrenaline, 448.1 ng/dl, 95% CI, 336.9–559.3, $p = 0.0711$), compared to the low N-inv group (mean CRP, 0.40 mg/dl, 95% CI, 0.14–0.65; mean noradrenaline, 326.3 ng/dl, 95% CI, 225.0–407.6).

### N-inv and activation of spinal cord astrocytes in patients with pancreatic cancer

Two autopsy cases without PVST around the SMA on CT images showed no N-inv around the SMA upon histological analysis. In contrast, two other autopsy cases in which PVST completely encircled the SMA were found to have severe extrapancreatic N-inv around the SMA. Damage to spinal nerves leads to activation of spinal cord astrocytes and microglia,[12,24] which can be identified by the expression of GFAP and Iba-1, respectively. Activated astrocytes showed hypertrophy and a larger GFAP-positive area. GFAP-positive cells in the spinal cords of the N-inv cases showed thickened branches and enlarged cell bodies, compared to the non-N-inv cases (Fig. 2*d*). Quantification of these morphological phenomena in the ipsilateral dorsal horn showed that the GFAP- and Iba-1-positive areas in N-inv patients were larger (4.2-fold, 2.0-fold, respectively) than those in the spinal cords of non-N-inv patients (Fig. 2*e*). These results were consistent with upregulation of GFAP (2.1-fold) and Iba-1 (5.8-fold) mRNA in the spinal cord as observed with real-time RT-PCR analysis (Supporting Information Fig. 2).

### Cachectic changes in the N-inv model

Pancreatic cancer cells in the left sciatic nerve of SCID mice formed a spindle tumor that extended proximally (Fig. 3*a*) and formed a ductal shape (stained by HE and cytokeratin AE1/3, Figs. 3*b* and 3*c*). N-inv mice resulting from injection of two pancreatic cancer cell lines, Capan-1 and BxPC-3, were produced. Compared to Capan-1-injected mice, mice given PBS ($n = 4$) and SC ($n = 8$) gained BW from 3 weeks later until the end of the experiment (6 week), compared to their original weights (Fig. 3*d* and Supporting Information Table 3). However, the BWs of the N-inv mice ($n = 8$) decreased from 3 to 6 week. The BW loss in the N-inv mice was obvious at 5 week ($-0.3 \pm 1.5$ g) and 6 week ($-0.5 \pm 0.7$ g), compared to the BW in the PBS ($1.4 \pm 1.1$ g, $p < 0.05$; $1.8 \pm 0.7$ g, $p < 0.01$, respectively) and SC mice ($1.4 \pm$

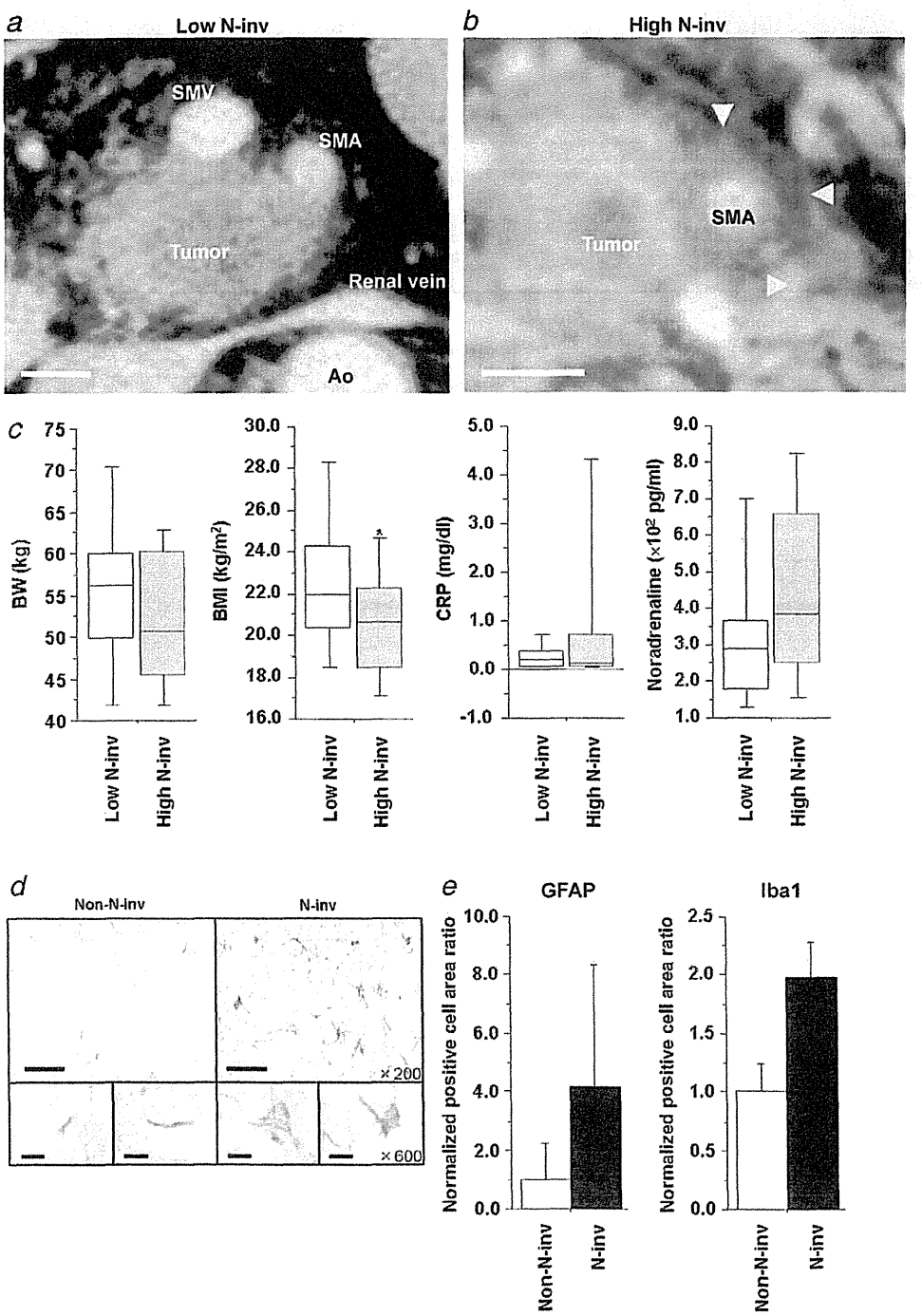


Figure 2. Body composition and spinal cord glial activation in patients with pancreatic cancer. (*a*) Patients with PVST that encircled neither the SMA and nor CeA completely were assigned to the low N-inv group. Scale bar: 10 mm. (*b*) High N-inv was defined as PVST encircling the SMA or CeA completely. The white arrowheads indicate the area of PVST. Scale bar: 10 mm. (*c*) The physical and clinical data before chemotherapy were compared between the low N-inv ($n = 26$) and the high N-inv patients ($n = 24$). (*d*) Spinal cord sections showing IHC and LFB staining obtained from autopsy tissues of patients with pancreatic cancer. The GFAP-positive cells in patients with extrapancreatic N-inv ($n = 2$) had thickened branches and enlarged cell bodies, compared to patients without extrapancreatic N-inv ($n = 2$). Top, scale bar: 50 μm. Bottom, scale bar: 10 μm. (*e*) GFAP-positive and Iba1-positive cell areas in the bilateral dorsal horn of Th10 and L1 were quantified. L1 was used as an internal standard. The ratios of Th10 to L1 are presented as the fold changes to non-N-inv patients. $^{*}p < 0.05$, $^{**}p < 0.01$. Median, 5th, 25th, 75th and 95th percentiles are presented as vertical boxes with error bars representing the lower and upper 5% margins. The results are expressed as the means ± standard deviations. SMA, superior mesenteric artery; SMV, superior mesenteric vein; Ao, aorta.

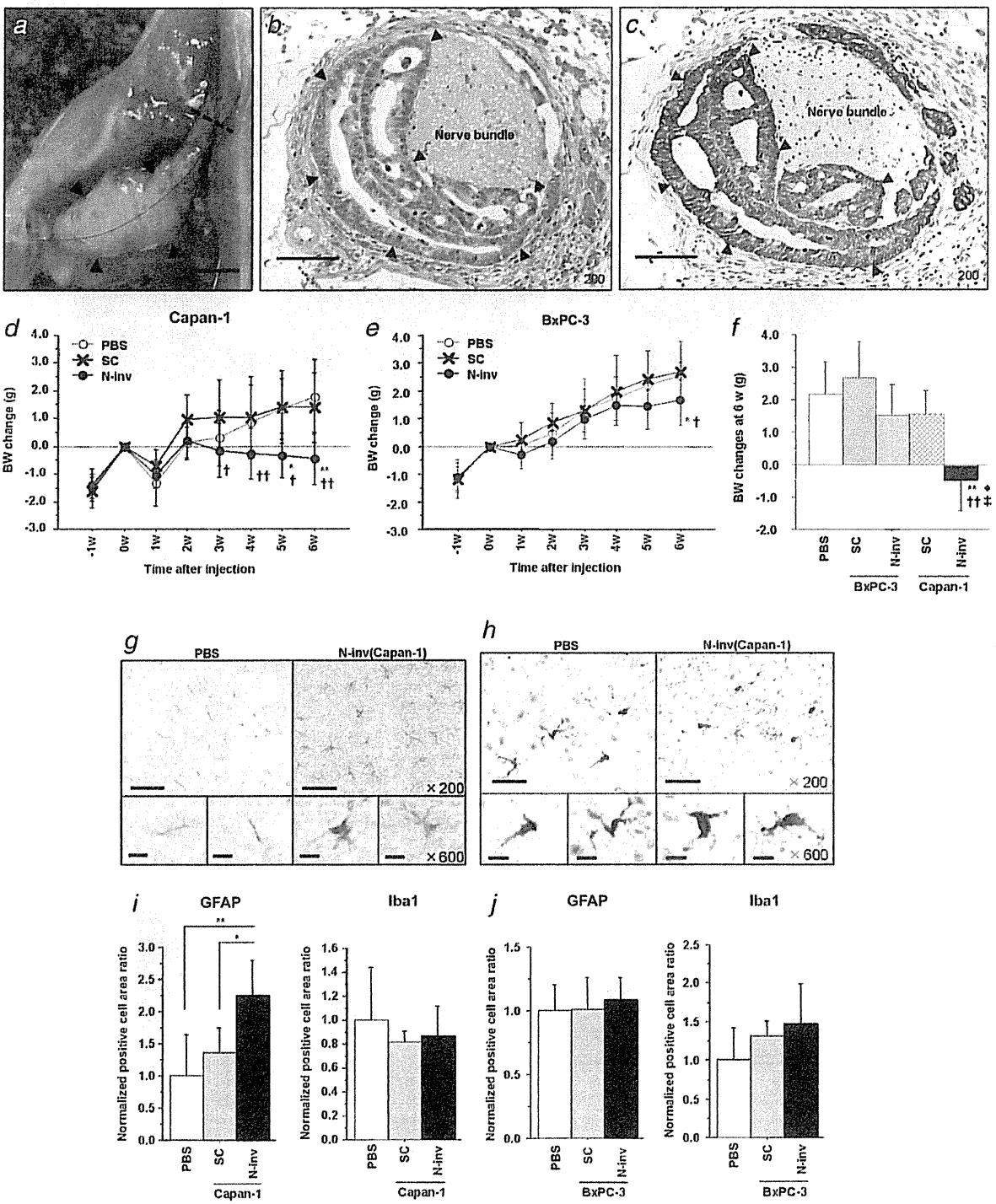


Figure 3. Cachectic changes in the N-inv model. (*a*) Macroscopic images of the left sciatic nerve in N-inv mice (Capan-1) at 6 week. Pancreatic cancer cells formed a spindle tumor (arrow head). Black curved line shows original left sciatic nerve. Scale bar: 5 mm. (*b*) Histological images of invasive pancreatic cancer cells were obtained at the level of the broken line in (*a*). Pancreatic cancer cells formed a ductal shape (arrow head) along the nerve bundle. Scale bar: 100 μm. (*c*) The same section as (*b*) was stained with cytokeratin AE1/3, an epithelial marker. Scale bar: 100 μm. (*d* and *e*) chronological BW changes from the original weight in PBS ($n = 4$ each), SC ($n = 8$, $n = 7$, respectively), and N-inv mice with Capan-1 cells ($n = 8$) (*d*) and BxPC-3 cells ($n = 7$) (*e*). $^{*}p < 0.05$, $^{**}p < 0.01$ *vs.* PBS mice; †$p < 0.05$, ††$p < 0.01$ *vs.* SC mice. (*f*) Total BW changes from the original weight at 6 week. $^{**}p < 0.01$ *vs.* PBS mice, ††$p < 0.01$ *vs.* SC (BxPC-3) mice, ◆$p < 0.05$ *vs.* N-inv (BxPC-3) mice, ‡$p < 0.05$, *vs.* SC (Capan-1) mice. (*g* and *h*) IHC images for GFAP (*g*) and Iba1 (*h*) in Th13 were taken from PBS and N-inv (Capan-1) mice at 6 week. Top, scale bar: 50 μm. Bottom, scale bar: 10 μm. (*i* and *j*) Quantification of the GFAP-positive and Iba1-positive cell area ratio in the ipsilateral dorsal horn relative to the N-inv in Th13 in mice given Capan-1 (*i*) and BxPC3 (*j*) cells. $^{*}p < 0.05$, $^{**}p < 0.01$. The ratios are presented as the fold changes relative to the PBS group. Data are expressed as the means ± standard deviation.

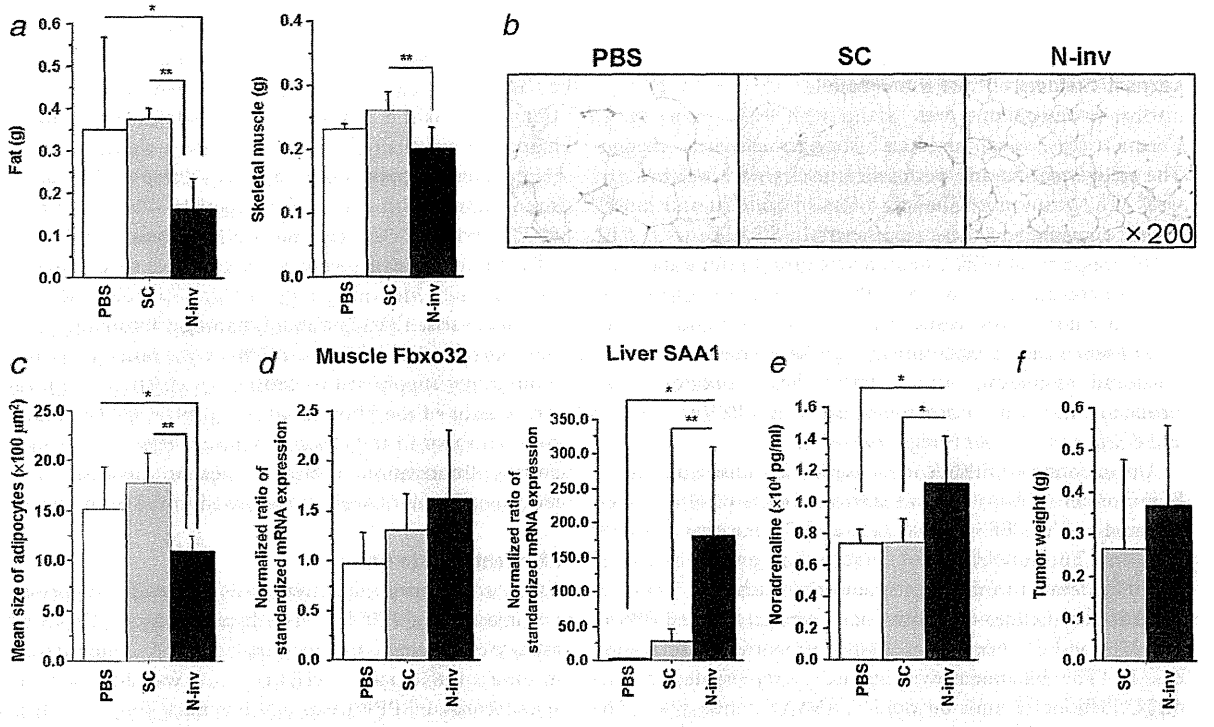


Figure 4. Cachectic features of the N-inv model (Capan-1). (*a* and *f*) Epididymal fat tissue, greater pectoral muscle and tumors were harvested and weighed at 6 week. (*b*) HE stained sections of epididymal adipose tissue from PBS ($n = 4$), SC ($n = 8$) and N-inv ($n = 8$) mice at 6 week were assessed with light microscopy. Scale bar: 50 μm. Adipocyte size, as determined by the sectional area, of N-inv mice was smaller than that in PBS and SC mice. (*c*) Adipocyte size in epididymal adipose tissue was quantified. (*d*) mRNA expression of Fbxo32 in muscle and SAA1 in liver at 6 week is shown. (*e*) The serum noradrenaline level at 6 week was measured with HPLC. *$p < 0.05$, **$p < 0.01$. mRNA expression of target genes normalized to GAPDH is presented as fold change to PBS mice. The results are expressed as the means ± standard deviations.

0.8 g, $p < 0.05$; 1.6 ± 0.9 g, $p < 0.01$, respectively). The BW of N-inv mice given BxPC-3 cells ($n = 7$) did not increase after 4 week, and the gain in BW (1.4 ± 0.9 g) was very small at 6 week, compared to that of mice given PBS ($n = 4$, 2.5 ± 0.5 g, $p < 0.05$) and SC ($n = 7$, 2.7 ± 1.1 g, $p < 0.05$) (Fig. 3*e*). N-inv mice given Capan-1 cells exhibited a marked BW loss at 6 week, compared to N-inv mice given BxPC-3 cells ($p < 0.05$) (Fig. 3*f*). No differences in food intake were observed among the three experimental groups for either Capan-1 or BxPC-3 cells (Supporting Information 1 and Table 4).

### Microarray analysis using spinal cords of N-inv mice

At the beginning of the evaluation of spinal cords from N-inv mice, microarray analysis was performed using the first lumbar cord (L1) from PBS, SC and N-inv mice with Capan-1 cells at 6 week ($n = 2$ each) (Supporting Information Table 2). Overexpressed genes in the N-inv mice at L1 included galanin, prodynorphin (PDYN) and GFAP. These genes are known to be upregulated in the spinal cord after injury to the spinal nerve.[24–26] The mRNA levels of these three genes evaluated with real-time RT-PCR at 6 week were higher in the spines of N-inv mice ($n = 2$) than those in the PBS ($n = 2$) and SC ($n = 1$) mice (Supporting Information Fig. 4). The damage caused by N-inv may be responsible for the elevation of galanin, PDYN and GFAP.

### Activation of astrocytes in the spinal cords of N-inv mice

Next, spinal cord glial activation was investigated with IHC and RT-PCR analyses. GFAP-positive cells in the spinal cords of N-inv mice with Capan-1 cells exhibited thickened branches and enlarged cell bodies, compared to mice given PBS (Fig. 3*g*). The GFAP-positive area in the N-inv mice was 2.2-fold larger than that in the spinal cords of PBS mice ($p < 0.01$) and 1.6-fold larger than that in the spinal cords of SC mice ($p < 0.05$) (Fig. 3*i*). Morphological features of Iba1-positive cells in the spinal cords did not show evident difference among three groups (Fig. 3*h*). Iba1-positive area was not significantly different among the PBS, SC and N-inv mice. These results were consistent with the mRNA expression of GFAP and Iba1 in the spinal cord (Supporting Information Fig. 2). In contrast, no obvious differences were observed in

the GFAP-positive areas among the three experimental groups given BxPC-3 cells (Fig. 3*j*).

### Cachectic features of the N-inv model

Further investigations were done with N-inv mice given Capan-1 cells, which produced stronger cachectic changes. The epididymal fat and pectoralis muscles were weighed at 6 week. The N-inv mice showed a loss of both fat and muscle weight compared to these parameters in SC mice ($p < 0.01$, <0.01, respectively) (Fig. 4*a* and Supporting Information Table 5). Between the N-inv and PBS mice, the weight loss in the N-inv mice was evident in the fat ($p < 0.05$) and tended to be lower in the skeletal muscle, but the difference was not statistically significant ($p = 0.095$). The adipocytes were smaller in the N-inv mice compared to the PBS ($p < 0.05$) and SC mice ($p < 0.01$) (Figs. 4*b* and 4*c*).

Upregulation of mRNA for a marker of muscle atrophy,[27] F-box protein (Fbxo) 32, was seen in muscle of N-inv mice, compared to the PBS ($p = 0.111$) and SC mice ($p = 0.283$) (Fig. 4*d*). The mRNA level of uncoupling protein (UCP) 2, which is elevated in muscle tissue during cachexia,[28] was elevated in the muscles of N-inv mice, compared to the PBS ($p = 0.178$) and SC mice ($p = 0.148$) (Supporting Information Fig. 3). The inflammatory response is represented by the mRNA level of serum amyloid A (SAA) in the liver. The SAA1 mRNA expression level in the N-inv mice was higher than that in the PBS ($p < 0.05$) and SC mice ($p < 0.01$) (Fig. 4*d*). The serum level of noradrenaline in the N-inv mice was significantly higher than that in the PBS ($p < 0.05$) and SC mice ($p < 0.05$) (Fig. 4*e*). The tumor weight was similar between the N-inv and SC mice at 6 week. The mean tumor weight in the N-inv mice was 0.37 ± 0.19 g, corresponding to 1.78% of the BW (Fig. 4*f*). BxPC-3 cells formed intraneural tumors that were smaller than those formed by Capan-1 cells (0.13 ± 0.09 g, data not shown).

### Ligation of the nerve route in N-inv mice

We ligated the proximal nerve to disrupt the connection between the N-inv and the CNS in N-inv mice given Capan-1 cells (Ligated N-inv mice or N-inv + ligation, $n = 5$). The BW changes in the ligated N-inv mice were similar to those in ligated PBS mice ($n = 4$), which were ligated at a site proximal to the PBS injection (Fig. 5*a* and Supporting Information Table 3). The BW loss in the N-inv mice ($n = 5$) and the increased BW of the PBS mice ($n = 3$) were reproducible. The BWs of the N-inv mice were markedly low at 5 week (−1.6 ± 1.1 g) and 6 week (−2.0 ± 1.3 g), compared to the PBS (2.0 ± 0.9 g, $p < 0.01$; 2.9 ± 0.8 g, $p < 0.01$), ligated PBS (1.0 ± 0.5 g, $p < 0.01$; 0.7 ± 0.9 g, $p < 0.01$) and ligated N-inv mice (1.0 ± 1.1 g, $p < 0.01$; 0.8 ± 1.1 g, $p < 0.01$, respectively). No significant differences were seen in food intake among the four groups during the observation period (Supporting Information Fig. 1 and Table 4). The activation of astrocytes in N-inv mice was reproducible in the experiments with ligation (Figs. 5*b*, 5*c* and Supporting Information Fig. 2). Hypertrophy, increased size of the GFAP cell area, and increased GFAP mRNA expression were observed in the N-inv mice and these GFAP changes were attenuated by the ligation of the sciatic nerve proximal to the N-inv. Compared to the N-inv mice, the ligated N-inv mice had higher fat weights ($p < 0.05$) and muscle weights ($p = 0.136$) (Fig. 5*d* and Supporting Information Table 5). The adipocyte size in ligated N-inv mice was larger than that in N-inv mice ($p < 0.05$) (Fig. 5*e*). The mean mRNA levels of Fbxo32 and UCP2 in the ligated N-inv mice tended to be lower than those in the N-inv mice ($p = 0.177$, $p = 0.288$, respectively) in muscle tissue (Fig. 5*f* and Supporting Information Fig. 3). The upregulation of SAA1 mRNA as a result of N-inv was significantly suppressed by ligation ($p < 0.01$). The mean tumor weight of the N-inv mice was 0.49 ± 0.09 g, which was similar to that in the other N-inv mice (Figs. 4*f*, 5*g* and Supporting Information Table 5). Ligation provided a 76.3% reduction in tumor weight, compared to the N-inv mice.

### PPF treatment in vivo

Spinal cord astrocytic activation is reportedly suppressed by i.p. injection of PPF.[14,29] The hypertrophy of GFAP-labeled astrocytes observed in the spinal cords of saline-treated N-inv mice with Capan-1 cells ($n = 3$) was attenuated in the spinal cords of PPF-treated N-inv mice ($n = 3$) (Fig. 6*b*). The GFAP-positive area in the spinal cord of PPF-treated N-inv mice was 44.1% smaller than that of saline-treated N-inv mice (Fig. 6*c*). PPF administration caused a 23.4% reduction in the mRNA expression of GFAP ($p = 0.089$) (Supporting Information Fig. 2). The BW of the PPF-treated N-inv mice had not decreased after 2 week, but the BW of the saline-treated mice began to decrease after 5 week. A significant difference in BW was observed between the saline-treated and PPF-treated N-inv mice at 6 week (Fig. 6*a* and Supporting Information Table 3). Food intake was similar in the two experimental groups (Supporting Information Fig. 1 and Table 4). The PPF-treated N-inv mice had a higher muscle tissue weight ($p = 0.0152$), compared to saline-treated N-inv mice. The differences in fat mass and tumor weight were not significantly different between the saline and PPF-treated N-inv mice (Fig. 6*d*, 6*g* and Supporting Information Table 5). The mean size of adipocytes in PPF-treated N-inv mice was similar to that in saline-treated N-inv mice (Fig. 6*e*). Fbxo32 and UCP2 mRNA levels in the muscles of PPF-treated N-inv mice were markedly reduced, compared to levels in saline mice ($p = 0.0792$, $p < 0.05$) (Fig. 6*f* and Supporting Information Fig. 3).

## Discussion

N-inv mice and patients with severe N-inv show a BW loss. Subcutaneous tumors and intraneural injection of PBS did not impact weight loss in mice. Intraneural tumors, but not extra-neural tumors or the manipulation of an intraneural injection, led to the reduction in body mass. A wasting condition with elevated inflammatory status is recognized as

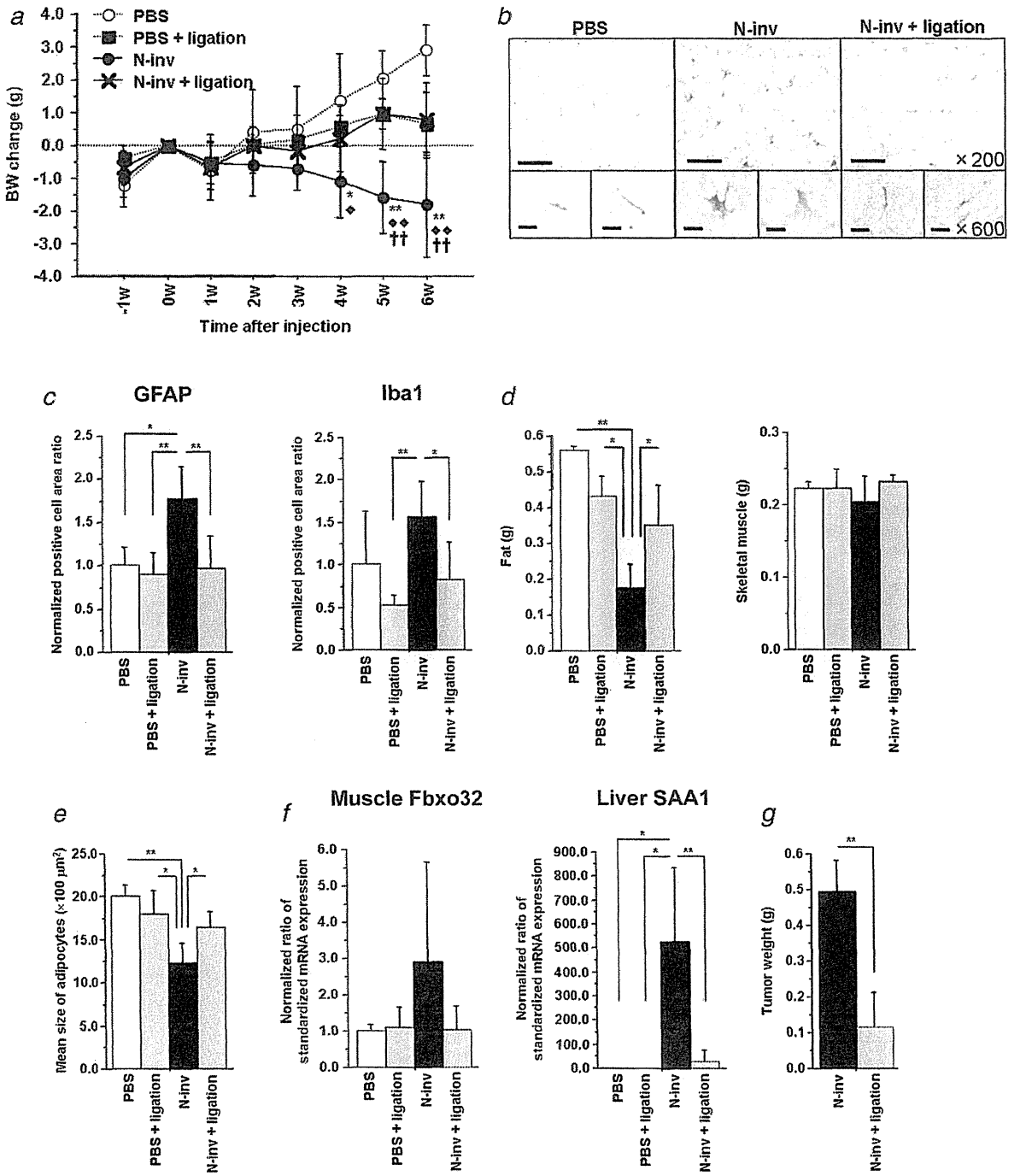


Figure 5. Ligation of the nerve route in N-inv mice (Capan-1). (*a*) Ligation of the sciatic nerve at a site proximal from the site of inoculation was performed in PBS ($n = 4$) and N-inv ($n = 5$) mice. Nonligated PBS ($n = 3$) and N-inv ($n = 5$) mice were used as controls. BW changes from the original weight were plotted weekly. $*p < 0.05$, $**p < 0.01$ *vs.* PBS group; $\blacklozenge p < 0.05$, $\blacklozenge\blacklozenge p < 0.01$ *vs.* ligated PBS group; $\dagger\dagger p < 0.01$ *vs.* ligated N-inv group. (*b*) The hypertrophic features of the GFAP-positive cells in the N-inv mice in Figure 3*g* were reproducibly observed in the N-inv mice at and were attenuated in the ligated N-inv mice. Top, scale bar: 50 μm. Bottom, scale bar: 10 μm. (*c*) Quantification of the GFAP-positive and Iba1-positive cell area ratio in the ipsilateral dorsal horn relative to the N-inv in Th13 was performed. (*d* and *g*) Fat, muscle and tumors were harvested and weighed at 6 week. (*e*) Adipocyte size in epididymal adipose tissue was calculated. (*f*) mRNA expression of Fbxo32 in muscle and SAA1 in liver at 6 week is shown. $*p < 0.05$, $**p < 0.01$. mRNA expression of target genes normalized to GAPDH is presented as fold changes to PBS group. The results are expressed as the means ± standard deviations.

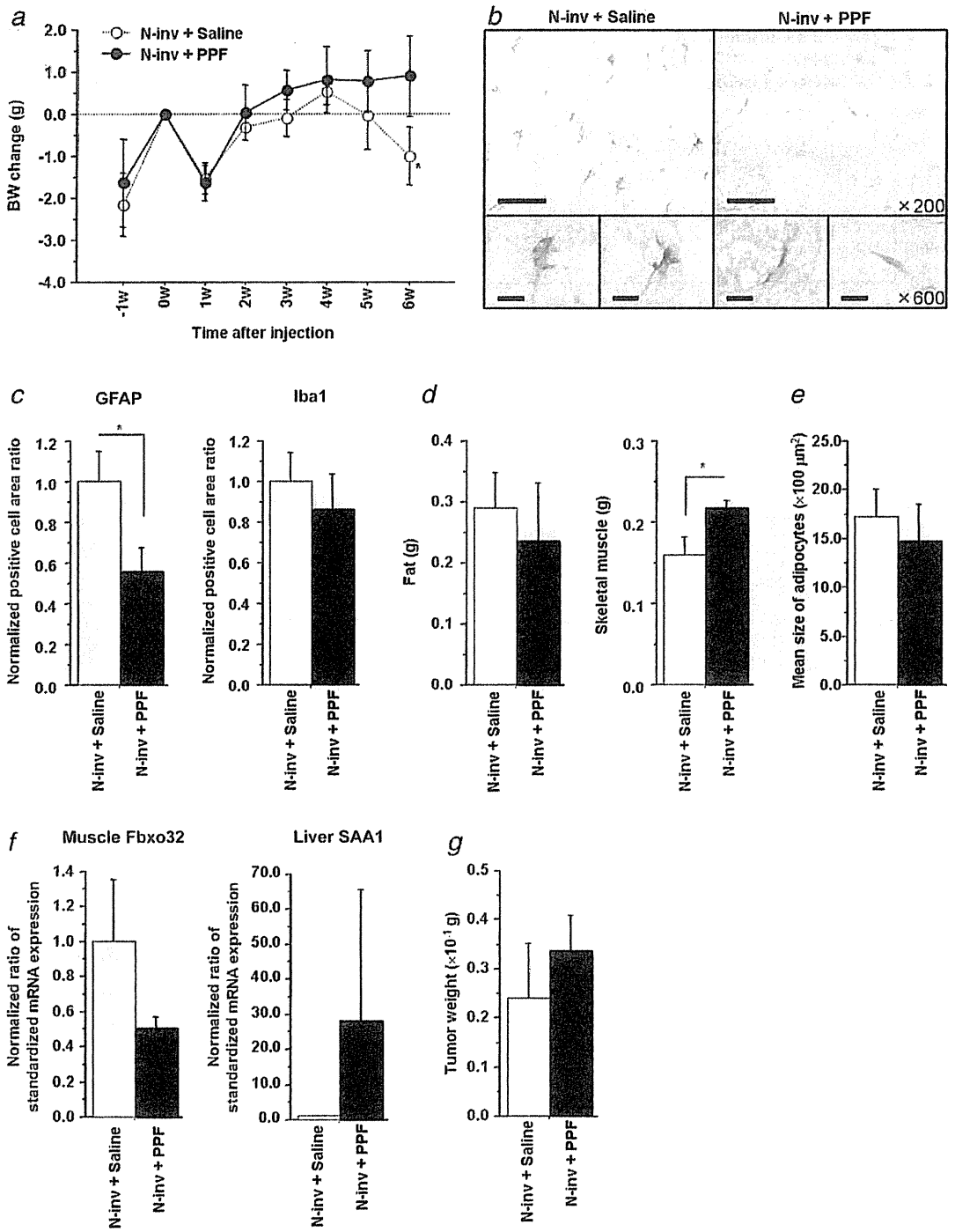


Figure 6. Effects of PPF in N-inv mice. (*a*) PPF (10 mg/kg) or the saline vehicle ($n = 3$/treatment) was administered to N-inv mice (Capan-1) by i.p. injection. The BW changes were then measured weekly. (*b*) IHC for GFAP in Th13 spinal cord dorsal horns showed that relatively thick GFAP-positive cells were seen in the saline group, but these cells were slimmer in the PPF group. Top, scale bar: 50 μm. Bottom, scale bar: 10 μm. (*c*) The GFAP-positive and Iba1-positive cell area ratios in the ipsilateral dorsal horns of N-inv were quantified. (*d* and *g*) The weights of the fat, muscle and tumors in each group at 6 week are shown. (*e*) Mean adipocyte size in epididymal fat was quantified. (*f*) mRNA expression of Fbxo32 in muscle and SAA1 in liver at 6 week was evaluated using real-time RT-PCR. $^*p < 0.05$. Positive cell area ratios and mRNA expression of target genes normalized to GAPDH are presented as the fold changes relative to the saline-treated N-inv group. The results are expressed as the means ± standard deviations.

cachexia.[20] Elevated SAA1 mRNA expression in liver and increased levels of circulating CRP were observed in N-inv mice and in patients with pancreatic cancer with high N-inv, respectively. Our study revealed that N-inv was a novel factor that induces cachexia in pancreatic cancer.

Cachexia involves catabolic changes in fat and muscle.[1] The body tissues that were decreased in N-inv mice were adipose and muscle tissue. Catabolic changes in muscle were reported after denervation or suppression of the activin receptor IIB in muscle due to upregulation of Fbxo32, a ubiquitin-protein ligase specific to muscle.[27,30,31] The increased mRNA level of Fbxo32 in the pectoral muscle in N-inv mice indicates the activation of muscle catabolism by N-inv. The loss of BMI, a good index of body fat,[32] in the high N-inv patients reinforced the idea that atrophy of adipose tissue was due to N-inv. Small lipid droplets and loss of fat mass were observed in N-inv mice. Noradrenaline induces lipolysis *via* adrenaline receptors and was elevated in the plasma of N-inv mice and the high N-inv patients.[33,34] These phenomena may indicate that lipolysis was due to N-inv. Anorexia is prevalent in patients with cachexia,[1] and this disorder affects lipid and amino acid metabolism.[35] Starvation results in fat and muscle catabolism.[36] The food intake in N-inv mice was similar to that in PBS and subcutaneous tumor model mice. The wasting condition of N-inv mice was independent of starvation. Experimental cachexia is preferably induced by a small amount of tumor (<5% of BW)[22] because the burden rarely exceeds 5% of the BW in patients with cancer.[37] In our N-inv mice injected with Capan-1 cells, the mean tumor weight was 1.78% of the BW. N-inv mice are a good model for cachexia regarding catalytic changes that are independent of calorie intake and that involve a small tumor burden.

Many studies have established that sciatic nerve ligation causes astrocytic activation in the spinal dorsal horn,[38,39] whereas our ligation experiment showed no obvious differences in the GFAP-positive areas between the PBS mice and ligated PBS mice. The difference in the observation period may be one possible explanation for this complication. Spinal cord astrocytes expression by sciatic nerve ligation was higher on 7 days than on 3 or 17 days in Andreea's study, suggesting that the peak of astrocytic activation by ligation was around day 7. Our observation period was much longer (42 days after ligation) than others and might be the phase after peak of astrocytic activation by sciatic nerve ligation. The persistent astrocytic activation in N-inv mice was likely due to repeated stimulation by tumor, compared to single stimulation by ligation.

N-inv mice injected with Capan-1 cells exhibited a marked BW loss and activation of spinal cord astrocytes compared to those injected with BxPC-3 cells. The differences between Capan-1- and BcPC-3-treated mice were a longer N-inv distance of Capan-1 cells than that of BxPC-3 cells,[21] mutations in KRAS and SMAD4, and many other factors.[40] We focused on the reaction of the host to N-inv and examined the status of astrocytic activation. The degree of astrocytic activation is mediated by damage to the peripheral nerve.[16] The spinal cords of human autopsy cases with N-inv also showed activation of spinal cord astrocytes compared to those without N-inv. The coexistence of N-inv and spinal cord glial activation was observed in both experimental and clinical N-inv. The activation of spinal cord astrocytes in N-inv mice was suppressed by ligation at a site proximal from the N-inv. The ligation of the sciatic nerve disrupted the transmission of the injury signal from the N-inv to the spinal cord. The neural damage signal caused by N-inv may mediate activation of astrocytes.

Systemic administration of PPF, a pan-phosphodiesterase (PDE) inhibitor, to N-inv mice suppressed the activation of spinal cord astrocytes and the loss of BW and skeletal muscle weight. PDE inhibitors downregulate the activation of astrocytes and microglia[14,29] and induce hypertrophy of skeletal muscle.[41] Another PDE inhibitor, pentoxifylline, failed to improve the appetite and BW loss in patients with cancer cachexia,[42] and the hypertrophic effect in muscle due to the PDE inhibitor was limited in cancer cachexia. Therefore, prevention of the wasting condition in N-inv mice by the PDE inhibitor implied a direct effect of PDE inhibition in muscle and an indirect effect due to suppression of astrocytic activation.

Mean relative level of SAA1 mRNA in PPF-treated group (5.2 ± 7.0) tends to be higher than that in saline-treated group (0.2 ± 0.0). Each values of SAA1 mRNA level in PPF group were extremely varied. We think this issue is difficult to discuss at present and interpret there is no significant difference between hepatic SAA1 mRNA level of PPF and vehicle group in our study. If hepatic SAA1 level truly tends to be elevated in PPF mice, a direct effect of PPF on hepatocyte is possibly associated with. The expressions of SAA1 mRNA and protein synthesis in hepatocytes are known to be mainly induced by inflammatory cytokines, such as IL-1, TNFα and IL-6.[43,44] Upregulation of SAA1 mRNA expression in PPF-treated N-inv mice may be due to a direct effect of PPF on hepatocyte, because increased intracellular cAMP leads to elevation of IL-6 production in hepatocyte.[45] The levels of cytokine and cAMP in hepatocyte were not examined in our study. Additional examinations are required to solve this issue.

The mechanism of astrocyte activation that subsequently causes cachexia was not examined in our study. Sympathetic activity may be a candidate. The mean level of blood noradrenaline, which is known to correlate with systemic sympathetic activity,[46] was high in severe N-inv patients and N-inv mice. Sympathetic activation induces lipolysis in adipose tissue[34] and muscle atrophy,[33,41] and thus causes BW loss. Because efferent fibers from the spinal cord to peripheral tissues include sympathetic nerves, spinal cord glial activation may affect sympathetic activity *via* neural routes. Astrocyte-derived cytokines are the other candidates. Astrocytic activation leads to the production and release of inflammatory cytokines, such as IL-1β, IL-6 and TNF-α.[47] IL-1 plays an

important role in lipid metabolism.[48] IL-6 and TNF-α are known to stimulate lipolysis in adipose tissue.[49] Astrocyte-derived cytokines are possible to induce lipolysis in adipose tissue in N-inv mice.

Our study has some limitations. First, a wide variety of effects of PPF made interpretation of our results complex. The combined action of PPF as a PDE inhibitor and a transporter of extracellular adenosine strengthens cyclic adenosine-5′,3′-monophosphate (cAMP) signaling.[29] Systemic administration of PPF to N-inv mice did not suppress the weight loss in adipose tissue. Stimulation of intracellular cAMP signaling leads to lipolysis in adipose tissue.[50] The failure to gain fat mass may have been caused by the lipolytic effect in adipose tissues, exceeding the downregulation of activated astrocytes in the spinal cord. Furthermore, the inhibitory effect of PPF on spinal cord microglial activation was not examined in this work, but should be investigated in the future. Finally, the difference in BW changes between N-inv mice and ligated N-inv mice was not evaluated under conditions of similar tumor weights. The reason for the decrease in tumor weights in N-inv mice by ligation was not examined in our study, but the reduction in intraneural tumors likely improved the cachectic changes. Further studies are required to examine the influences of ligation on the environment around the tumor, including neurotrophic factors.

In conclusion, our study showed (1) characteristics of cachexia by N-inv in patients with pancreatic cancer and in an experimental mouse model, (2) a relationship between N-inv and spinal cord astrocytic activation *via* a neural route in patients with pancreatic cancer and the experimental mouse model and (3) the anti-cachectic effect of suppression of spinal cord astrocytic activation in the experimental model. This is the first evidence that spinal cord astrocytes mediate cancer cachexia *via* neural routes. In addition, the cachectic animal model induced by N-inv has been established for the first time. Future studies on N-inv and spinal cord glial activation may provide insight into strategies for anti-cachectic therapy.



## References


1. Tisdale MJ. Cancer cachexia. *Langenbecks Arch Surg* 2004;389:299–305.
2. Dewys WD, Begg C, Lavin PT, et al. Prognostic effect of weight loss prior to chemotherapy in cancer patients. Eastern Cooperative Oncology Group. *Am J Med* 1980;69:491–7.
3. Ikeda M, Okada S, Tokuuye K, et al. Prognostic factors in patients with locallyadvanced pancreatic carcinoma receiving chemoradiotherapy. *Cancer* 2001;91:490–5.
4. Nieto J, Grossbard ML, Kozuch P. Metastatic pancreatic cancer 2008: is the glass less empty? *Oncologist* 2008;13:562–76.
5. Bachmann J, Ketterer K, Marsch C, et al. Pancreatic cancer related cachexia: influence on metabolism and correlation to weight loss and pulmonary function. *BMC Cancer* 2009;9:255.
6. Bibby MC, Double JA, Ali SA, et al. Characterization of a transplantable adenocarcinoma of the mouse colon producing cachexia in recipient animals. *J Natl Cancer Inst* 1987;78:539–46.
7. Mitsunaga S, Hasebe T, Kinoshita T, et al. Detail histologic analysis of nerve plexus invasion in invasive ductal carcinoma of the pancreas and its prognostic impact. *Am J Surg Pathol* 2007;31:1636–44.
8. Mitsunaga S, Kinoshita T, Hasebe T, et al. Low serum level of cholinesterase at recurrence of pancreatic cancer is a poor prognostic factor and relates to systemic disorder and nerve plexus invasion. *Pancreas* 2008;36:241–8.
9. Bockman DE, Buchler M, Beger HG. Interaction of pancreatic ductal carcinoma with nerves leads to nerve damage. *Gastroenterology* 1994;107:219–30.
10. Ceyhan GO, Bergmann F, Kadihasanoglu M, et al. Pancreatic neuropathy and neuropathic pain–a comprehensive pathomorphological study of 546 cases. *Gastroenterology* 2009;136:177–86 e1.
11. Rutkowski MD, Winkelstein BA, Hickey WF, et al. Lumbar nerve root injury induces central nervous system neuroimmune activation and neuroinflammation in the rat: relationship to painful radiculopathy. *Spine* 2002;27:1604–13.
12. Hashizume H, DeLeo JA, Colburn RW, et al. Spinal glial activation and cytokine expression after lumbar root injury in the rat. *Spine* 2000;25:1206–17.
13. Gwak YS, Crown ED, Unabia GC, et al. Propentofylline attenuates allodynia, glial activation and modulates GABAergic tone after spinal cord injury in the rat. *Pain* 2008;138:410–22.
14. Sweitzer SM, Schubert P, DeLeo JA. Propentofylline, a glial modulating agent, exhibits antiallodynic properties in a rat model of neuropathic pain. *J Pharmacol Exp Ther* 2001;297:1210–7.
15. Tanga FY, Nutile-McMenemy N, DeLeo JA. The CNS role of Toll-like receptor 4 in innate neuroimmunity and painful neuropathy. *Proc Natl Acad Sci USA* 2005;102:5856–61.
16. Feng QX, Wang W, Feng XY, et al. Astrocytic activation in thoracic spinal cord contributes to persistent pain in rat model of chronic pancreatitis. *Neuroscience* 2010;167:501–9.
17. Neusch C, Bahr M, Schneider-Gold C. Glia cells in amyotrophic lateral sclerosis: new clues to understanding an old disease? *Muscle Nerve* 2007;35:712–24.
18. Papadimitriou D, Le Verche V, Jacquier A, et al. Inflammation in ALS and SMA: sorting out the good from the evil. *Neurobiol Dis* 2010;37:493–502.
19. Fukuda T, Iwanaga S, Sakamoto I, et al. CT of neural plexus invasion in common bile duct carcinoma. *J Comput Assist Tomogr* 1998;22:351–6.
20. Evans WJ, Morley JE, Argiles J, et al. Cachexia: a new definition. *Clin Nutr* 2008;27:793–9.
21. Mitsunaga S, Fujii S, Ishii G, et al. Nerve invasion distance is dependent on laminin gamma2 in tumors of pancreatic cancer. *Int J Cancer* 2010;127:805–19.
22. Tisdale MJ. Cancer cachexia. *Br J Cancer* 1991;63:337–42.
23. Bujalska IJ, Hewitt KN, Hauton D, et al. Lack of hexose-6-phosphate dehydrogenase impairs lipid mobilization from mouse adipose tissue. *Endocrinology* 2008;149:2584–91.
24. Hald A, Nedergaard S, Hansen RR, et al. Differential activation of spinal cord glial cells in murine models of neuropathic and cancer pain. *Eur J Pain* 2009;13:138–45.
25. Obara I, Mika J, Schafer MK, et al. Antagonists of the kappa-opioid receptor enhance allodynia in rats and mice after sciatic nerve ligation. *Br J Pharmacol* 2003;140:538–46.
26. Zhang X, Xu ZO, Shi TJ, et al. Regulation of expression of galanin and galanin receptors in dorsal root ganglia and spinal cord after axotomy and inflammation. *Ann NY Acad Sci* 1998;863:402–13.
27. Bodine SC, Latres E, Baumhueter S, et al. Identification of ubiquitin ligases required for skeletal muscle atrophy. *Science* 2001;294:1704–8.
28. Gordon JN, Green SR, Goggin PM. Cancer cachexia. *QJM* 2005;98:779–88.
29. Ringheim GE. Glial modulating and neurotrophic properties of propentofylline and its application to Alzheimer's disease and vascular dementia. *Ann NY Acad Sci* 2000;903:529–34.
30. Hinkle RT, Dolan E, Cody DB, et al. Phosphodiesterase 4 inhibition reduces skeletal muscle atrophy. *Muscle Nerve* 2005;32:775–81.
31. Gomes MD, Lecker SH, Jagoe RT, et al. Atrogin-1, a muscle-specific F-box protein highly expressed during muscle atrophy. *Proc Natl Acad Sci USA* 2001;98:14440–5.
32. Gallagher D, Visser M, Sepulveda D, et al. How useful is body mass index for comparison of body fatness across age, sex, and ethnic groups? *Am J Epidemiol* 1996;143:228–39.
33. Qvisth V, Hagstrom-Toft E, Enoksson S, et al. Human skeletal muscle lipolysis is more responsive to epinephrine than to norepinephrine stimulation in vivo. *J Clin Endocrinol Metab* 2006;91:665–70.
34. Dodt C, Lonnroth P, Wellhoner JP, et al. Sympathetic control of white adipose tissue in

lean and obese humans. *Acta Physiol Scand* 2003; 177:351–7.
35. Esper DH, Harb WA. The cancer cachexia syndrome: a review of metabolic and clinical manifestations. *Nutr Clin Pract* 2005;20:369–76.
36. Cahill GF,Jr. Starvation in man. *Clin Endocrinol Metab* 1976;5:397–415.
37. Waterhouse C. How tumors affect host metabolism. *Ann NY Acad Sci* 1974;230:86–93.
38. Xu M, Bruchas MR, Ippolito DL, et al. Sciatic nerve ligation-induced proliferation of spinal cord astrocytes is mediated by kappa opioid activation of p38 mitogen-activated protein kinase. *J Neurosci* 2007;27:2570–81.
39. Bura SA, Nadal X, Ledent C, et al. A 2A adenosine receptor regulates glia proliferation and pain after peripheral nerve injury. *Pain* 2008;140: 95–103.
40. Deer EL, Gonzalez-Hernandez J, Coursen JD, et al. Phenotype and genotype of pancreatic cancer cell lines. *Pancreas* 2010;39:425–35.
41. Lynch GS, Ryall JG. Role of beta-adrenoceptor signaling in skeletal muscle: implications for muscle wasting and disease. *Physiol Rev* 2008;88: 729–67.
42. Goldberg RM, Loprinzi CL, Mailliard JA, et al. Pentoxifylline for treatment of cancer anorexia and cachexia? A randomized, double-blind, placebo-controlled trial. *J Clin Oncol* 1995;13: 2856–9.
43. Uhlar CM, Whitehead AS. The kinetics and magnitude of the synergistic activation of the serum amyloid A promoter by IL-1 beta and IL-6 is determined by the order of cytokine addition. *Scand J Immunol* 1999;49: 399–404.
44. Uhlar CM, Whitehead AS. Serum amyloid A, the major vertebrate acute-phase reactant. *Eur J Biochem* 1999;265:501–23.
45. Zidek Z. Adenosine—cyclic AMP pathways and cytokine expression. *Eur Cytokine Netw* 1999;10: 319–28.
46. Leimbach WN Jr, Wallin BG, Victor RG, et al. Direct evidence from intraneural recordings for increased central sympathetic outflow in patients with heart failure. *Circulation* 1986;73: 913–9.
47. Nakagawa T, Kaneko S. Spinal astrocytes as therapeutic targets for pathological pain. *J Pharmacol Sci* 2010;114:347–53.
48. Matsuki T, Horai R, Sudo K, et al. IL-1 plays an important role in lipid metabolism by regulating insulin levels under physiological conditions. *J Exp Med* 2003;198:877–88.
49. Ji C, Chen X, Gao C, et al. IL-6 induces lipolysis and mitochondrial dysfunction, but does not affect insulin-mediated glucose transport in 3T3-L1 adipocytes. *J Bioenerg Biomembr* 2011;43: 367–75.
50. Collins S, Surwit RS. The beta-adrenergic receptors and the control of adipose tissue metabolism and thermogenesis. *Recent Prog Horm Res* 2001;56:309–28.

Cancer Chemother Pharmacol (2012) 69:957–964
DOI 10.1007/s00280-011-1786-6

ORIGINAL ARTICLE

# Phase I/II study of gemcitabine as a fixed dose rate infusion and S-1 combination therapy (FGS) in gemcitabine-refractory pancreatic cancer patients

**Chigusa Morizane · Takuji Okusaka · Hideki Ueno · Shunsuke Kondo · Masafumi Ikeda · Junji Furuse · Ohkawa Shinichi · Kohei Nakachi · Shuichi Mitsunaga · Yasushi Kojima · Eiichiro Suzuki · Makoto Ueno · Tomohiro Yamaguchi**

Received: 11 June 2011 / Accepted: 8 November 2011 / Published online: 26 November 2011


**Abstract**
*Purpose* There is no standard regimen for gemcitabine (Gem)-refractory pancreatic cancer (PC) patients. In a previous phase II trial, S-1 was found to exhibit marginal efficacy. Gem administration by fixed dose rate infusion of 10 mg/m$^2$/min (FDR-Gem) should maximize the rate of intracellular accumulation of gemcitabine triphosphate and might improve clinical efficacy. We conducted the phase I/II of FDR-Gem and S-1 (FGS) in patients with Gem-refractory PC.
*Methods* The patients received FDR-Gem on day 1 and S-1 orally twice daily on days 1–7. Cycles were repeated every 14 days. Patients were scheduled to receive Gem (mg/m$^2$/week) and S-1 (mg/m$^2$/day) at four dose levels in the phase I: 800/80 (level 1), 1,000/80 (level 2), 1,200/80 (level 3) and 1,200/100 (level 4). Forty patients were enrolled in the phase II study at recommended dose.
*Results* The recommended dose was the level 3. In the phase II, a partial response has been confirmed in seven patients (18%). The median overall survival time and median progression-free survival time are 7.0 and 2.8 months, respectively. The common adverse reactions were anorexia, leukocytopenia and neutropenia.
*Conclusion* This combination regimen of FGS is active and well tolerated in patients with Gem-refractory PC.

**Keywords** Chemotherapy · Pancreatic carcinoma · Second-line · Gemcitabine · S-1 · Salvage · Fixed dose rate infusion

## Introduction

Gemcitabine monotherapy or gemcitabine-containing combination chemotherapy is the standard first-line therapy for advanced pancreatic cancer. In the recent phase III study, the first-line FOLFIRINOX regimen (5-fluorouracil, leucovorin, irinotecan and oxaliplatin) led to a median survival of 11.1 months compared with 6.8 months in the gemcitabine group [4]. However, the FOLFIRINOX regimen was quite toxic (e.g., 5.4% of patients had grade 3 or 4 febrile neutropenia), and a survival benefit was shown only among a highly select population with a good performance status, an age of 75 years or younger, and normal or nearly normal bilirubin levels [13]. Therefore, this combination therapy was considered to be one of the treatment options for patients in good general condition, and gemcitabine remains the mainstay of care for patients with advanced pancreatic cancer. However, after disease progression during first-line gemcitabine-containing chemotherapy, the

The registration number of this clinical trial is UMIN ID, C000000450.

C. Morizane (✉) · T. Okusaka · H. Ueno · S. Kondo · T. Yamaguchi
Division of Hepatobiliary and Pancreatic Oncology, National Cancer Center Hospital, 5-1-1 Tsukiji, Chuo-ku, Tokyo 104-0045, Japan
e-mail: cmorizan@ncc.go.jp

M. Ikeda · K. Nakachi · S. Mitsunaga · Y. Kojima
Division of Hepatobiliary and Pancreatic Oncology, National Cancer Center Hospital, East, Kashiwa, Japan

J. Furuse · E. Suzuki
Division of Medical Oncology, Kyorin University School of Medicine, Tokyo, Japan

O. Shinichi · M. Ueno
Division of Hepatobiliary and Pancreatic Oncology, Kanagawa Cancer Center, Yokohama, Japan

options for further anticancer treatment are limited. S-1 is an orally administered anticancer drug that consists of a combination of tegafur, 5-chloro-2,4-dihydroxypyridine and oteracil potassium in a 1 : 0.4 : 1 molar ratio [27]. The antitumor effect of S-1 has already been demonstrated in a variety of solid tumors including pancreatic cancer [7, 11, 12, 14, 20, 21, 25, 26, 32, 33]. In patients with chemo-naïve pancreatic cancer, an overall response rate of 21.1% was achieved, and the median time-to-progression and median overall survival period were 3.7 and 8.3 months, respectively [32]. In gemcitabine-refractory metastatic pancreatic cancer, our recent phase II study of S-1 yielded results that demonstrated marginal activity including a response rate of 15%, a median progression-free survival time of 2.0 months and a median overall survival time of 4.5 months, with a favorable toxicity profile [17]. In addition, other reports also demonstrated marginal antitumor activity [1, 28]. Gemcitabine administration via infusion at a fixed dose rate of 10 mg/m$^2$/min (FDR-Gem) has been found to increase the intracellular drug concentrations, compared with gemcitabine at a standard dose rate infusion over a period of 30 min. A recent phase II study of combination therapy consisting of FDR-Gem and oxaliplatin (GEMOX) yielded results that demonstrated activity in gemcitabine-refractory advanced pancreatic cancer [5], although oxaliplatin is inactive against pancreatic cancer when used as a single agent [6]. The increased intracellular concentrations of gemcitabine as a result of FDR infusion and/or the synergistic effect of gemcitabine and oxaliplatin may play an important role in the antitumor effect of GEMOX. This finding is of interest when considering the effect of combination therapy consisting of FDR-Gem and some other agent that exhibits a synergistic effect with gemcitabine in patients with metastatic pancreatic cancer who failed standard dose rate gemcitabine.

The inhibition of ribonucleotide reductase by gemcitabine is considered to enhance the effect of the 5-FU metabolite 5-FdUMP by reducing the concentration of its physiological competitor [10]. Preclinical studies have demonstrated a synergy between gemcitabine and 5-FU in tumor cell lines, including pancreatic cancer cells [3, 23]. S-1 is a fluoropyrimidine, and several phase II studies of S-1 and gemcitabine combination therapy have yielded results that demonstrated a promising activity in chemo-naïve advanced pancreatic cancer patients, including a response rate of 32–48% and a median survival times of 7.89–12.5 months [16, 18, 19, 31].

Therefore, we conducted the present phase I/II study to determine the recommended doses of FDR-Gem and S-1 (FGS) to use for combination therapy and to evaluate the toxicity and efficacy at the recommended doses in patients with gemcitabine-refractory pancreatic cancer.

## Materials and methods

### Eligibility criteria

The eligibility criteria were histologically proven pancreatic adenocarcinoma with measurable metastatic lesions, disease progression during gemcitabine-based first-line chemotherapy, age 20 years or over, ECOG performance status of 0–2 points, more than 2-week interval between the final dose of the prior chemotherapy regimen and study entry, adequate bone marrow function (leukocyte count $\geq$ 3,500/mm$^3$, neutrophil count $\geq$ 1,500/mm$^3$, platelet count $\geq$ 100,000/mm$^3$, hemoglobin concentration $\geq$ 9.0 g/dL), adequate renal function (serum creatinine level $\leq$ 1.1 mg/dL) and adequate liver function (serum total bilirubin level $\leq$ 2.0 mg/dL, transaminase levels $\leq$ 100 U/L). Patients with obstructive jaundice or liver metastasis were considered eligible if their total bilirubin level $\leq$ 3.0 mg/dL and transaminase levels could be reduced to 150 U/L by biliary drainage. The exclusion criteria were regular use of phenytoin, warfarin or flucytosine, history of fluorinated pyrimidine use, severe mental disorder, active infection, ileus, watery diarrhea, interstitial pneumonitis or pulmonary fibrosis, refractory diabetes mellitus, heart failure, renal failure, active gastric or duodenal ulcer, massive pleural or abdominal effusion, brain metastasis, and active concomitant malignancy. Pregnant or lactating women were also excluded. Written informed consent was obtained from all patients. This study was approved by the institutional review board of the National Cancer Center of Japan.

### Treatment

Considering the patients' quality of life, we adopted biweekly schedule. Gemcitabine (Eli Lilly Japan K.K., Kobe, Japan) was administered by FDR intravenous infusion of 10 mg/m$^2$/min on day 1. S-1 (Taiho Pharmaceutical Co., Ltd., Tokyo, Japan) was administered orally twice daily on day 1 to day 7, followed by a 1-week rest. Treatment cycles were repeated every 2 weeks until disease progression or unacceptable toxicity occurred. If blood examination revealed leukocytopenia < 2,000/mm$^3$, thrombocytopenia < 75,000/mm$^3$, total bilirubin > 3.0 mg/dL, aspartate aminotransferase or alanine aminotransferase level > 150 U/L, or creatinine > 1.5 mg/dL, both gemcitabine and S-1 were withheld until recovery. If a patient experienced dose-limiting toxicity (DLT), the dose of gemcitabine and S-1 was reduced by one level in the subsequent cycle. If a rest period of more than 15 days was required because of toxicity, the patient was withdrawn from the study. Patients were scheduled to receive gemcitabine and S-1 at four dosage levels (Table 1). Two dosage levels of S-1 were established according to the body

**Table 1** Dosage levels of gemcitabine and S-1

| Dosage level | Gemcitabine | S-1 |
|---|---|---|
| Level 0 | 600 mg/m$^2$/60 min | Dosage A |
| Level 1[a] | 800 mg/m$^2$/80 min | Dosage A |
| Level 2 | 1,000 mg/m$^2$/100 min | Dosage A |
| Level 3 | 1,200 mg/m$^2$/120 min | Dosage A |
| Level 4 | 1,200 mg/m$^2$/120 min | Dosage B |

[a] Starting dosage

surface area as dosage A, about 80 mg/m$^2$/day, and dosage B, about 100 mg/m$^2$/day (Table 2). At the first dose level (level 1), gemcitabine was administered at a dosage of 800 mg/m$^2$ administered as a 80-min infusion, and S-1 was administered at dosage A. At the next dose level (level 2), the gemcitabine dosage was increased to 1,000 mg/m$^2$ administered as a 100-min infusion, and S-1 was administered at the same dosage. At the next dose level (level 3), the gemcitabine dosage was increased to 1,200 mg/m$^2$ administered as a 120-min infusion, and S-1 was administered at the same dosage. At the final dosage level (level 4), gemcitabine administered at the same dosage, and S-1 was administered at dosage B.

### Study design

This study was an open-label, four-center, single-arm phase I/II study performed in two steps. The objective of step 1 (phase I) was to evaluate the frequency of DLT during first 2 cycles (4 weeks) and then use the frequency of DLT to determine which of the four dosages tested to recommend (Table 1). At least 3 patients were enrolled at each dosage level. If DLT was observed in the initial three patients, up to three additional patients were entered at the same dosage level. The highest dosage level that did not cause DLT in 3 of the 3 or $\geq$3 of the 6 patients treated at that level during the first two cycles of treatment was considered the maximum-tolerated dosage (MTD). DLT was defined as (1) grade 4 leucopenia or grade 4 neutropenia or febrile neutropenia, (2) grade 4 thrombocytopenia or thrombocytopenia requiring transfusion, (3) grade 3 or 4 non-hematological toxicity excluding hyperglycemia and electrolyte disturbances, (4) serum transaminases levels, $\gamma$-glutamyl transpeptidase level and alkaline phosphatase level $\geq$10 times UNL, (5) serum creatinine level $\geq$ 2.0 mg/dL and (6) any toxicity that necessitated a treatment delay of more than 15 days. Toxicity was graded according to the Common Terminology Criteria for Adverse Events (CTCAE) version 3.0. In step 2, the recommended dosages (RD) of FGS were then administered, and the effect of this combination therapy on objective tumor response was evaluated in patients who were given the RD (phase II). The number of patients to be enrolled in phase II was determined by using a SWOG's standard design (attained design) [8, 9]. The phase II included the patients who received the RD in the step 1. The null hypothesis was that the overall response rate would be $\leq$5%, and the alternative hypothesis was that the overall response rate would be $\geq$20%. The $\alpha$ error was 5% (one-tailed), and the $\beta$ error was 10% (one-tailed). The alternative hypothesis was established based on the preferable data in previous reports [5, 15, 24, 30, 34]. Interim analysis was planned when 20 patients were enrolled. If none of the first 20 patients had a partial response or complete response, the study was to be ended. If a response was detected in any of the first 20 patients, an additional 20 patients were to be included in a second stage of accrual to more precisely estimate the actual response rate. If the number of objective responses after completing the trial was 5 or more among the 40 patients, then we would reject the null hypothesis and conclude that FGS was effective, and we would proceed to the next large-scale study. The severity of adverse events and progression-free survival and overall survival were investigated as secondary objectives in phase II.

**Table 2** Dosage of S-1 (tegafur equivalent)

| Body surface area (m$^2$) | Dosage A ($\fallingdotseq$80 mg/m$^2$/day) | Dosage B ($\fallingdotseq$100 mg/m$^2$/day) |
|---|---|---|
| <1.25 | 40 mg × 2/day | 50 mg × 2/day |
| 1.25–<1.5 | 50 mg × 2/day | 60 mg × 2/day |
| $\geq$1.5 | 60 mg × 2/day | 75 mg × 2/day |

## Results

### Patient characteristics

Between June 2006 and March 2009, 49 patients were enrolled in this study. Fifteen patients (level 1: 3 patients, level 2: 3 patients, level 3: 6 patients, level 4: 3 patients) were enrolled into the phase I (STEP 1), and an additional 34 patients were enrolled into the phase II (STEP2) at dose level 3. Table 3 shows the baseline characteristics of the patients in step 1 and step 2. A total of the 40 patients who were given the recommended dose, 6 patients and 34 patients who entered into the study at phase I and phase II, respectively, were evaluated for efficacy and detailed safety profile.

#### *Phase I (STEP 1)*

No DLT occurred during the first 2 cycles (4 weeks) at level 1 or level 2. At dose level 3, three patients were

**Table 3** Patient characteristics

| Characteristic | Step 1 | | | | Step 2 | Total at the recommended dose (level 3) |
|---|---|---|---|---|---|---|
| | Level 1 | Level 2 | Level 3 | Level 4 | Level 3 | |
| No. of patients | 3 | 3 | 6 | 3 | 34 | 40 |
| Age, years | | | | | | |
| Median | 66 | 58 | 64 | 62 | 63.5 | 64 |
| Range | 55–69 | 51–58 | 48–71 | 52–70 | 40–80 | 40–80 |
| Sex, *n* (%) | | | | | | |
| Male | 1 (33) | 3 (100) | 4 (67) | 1 (33) | 19 (56) | 23 (58) |
| Female | 2 (67) | 0 | 2 (33) | 2 (67) | 15 (44) | 17 (48) |
| ECOG performance status, *n* (%) | | | | | | |
| 0 | 2 (67) | 2 (67) | 5 (83) | 2 (67) | 22 (65) | 27 (68) |
| 1 | 1 (33) | 1 (33) | 1 (17) | 1 (33) | 12 (35) | 13 (33) |
| Primary tumor, *n* (%) | | | | | | |
| Head | 1 (33) | 2 (67) | 2 (33) | 2 (67) | 17 (50) | 19 (48) |
| Body/tail | 2 (67) | 1 (33) | 4 (67) | 1 (33) | 17 (50) | 21 (53) |
| Metastatic site, *n* (%) | | | | | | |
| Liver | 3 (100) | 3 (100) | 6 (100) | 1 (33) | 25 (74) | 31 (78) |
| Lung | 1 (33) | 0 | 0 | 2 (67) | 7 (21) | 7 (18) |
| Peritoneum | 1 (33) | 1 (33) | 0 | 1 (33) | 11 (32) | 11 (28) |
| Lymph node | 0 | 2 (67) | 0 | 0 | 11 (32) | 11 (28) |
| Tumor stage at the start of prior treatment, *n* (%) | | | | | | |
| Locally advanced | 0 | 0 | 0 | 1 (33) | 7 (21) | 7 (18) |
| Metastatic | 3 (100) | 3 (100) | 6 (100) | 2 (67) | 27 (79) | 33 (83) |
| Prior treatment, *n* (%) | | | | | | |
| Gemcitabine alone | 3 (100) | 3 (100) | 5 (83) | 3 (100) | 26 (76) | 31 (78) |
| Gem + Axitinib | 0 | 0 | 0 | 0 | 2 (6) | 2 (5) |
| Gem + Erlotinib | 0 | 0 | 1 (17) | 0 | 6 (18) | 7 (18) |

evaluated first, and none developed DLT. Since all 3 patients experienced DLT at dose level 4 (grade 4 neutropenia in two patients, grade 3 stomatitis in one patient), 3 additional patients were evaluated at dose level 3. A DLT (grade 4 neutropenia) was experienced by 2 of the 3 patients in this additional cohort in dose level 3, and dose level 3 was determined to be the MTD. Based on these results, the RD was determined to be level 3.

*Phase II (efficacy and safety profile in the 40 patients treated at dose level 3)*

In step 2, the RD of FDR-Gem and S-1 was administered to an additional 34 patients, and a total 40 patients were treated at dose level 3 to evaluate the objective tumor response to this combination therapy. As of the date of the analysis, the protocol treatment had been concluded in 39 of the 40 patients, and a total of 286 courses (median: 5 courses; range 1–31 courses) had been administered at level 3. The actual mean weekly dose administered were gemcitabine 545 mg/m$^2$/week (90.8% of planned dosage) and 90.1% of planned dosage of S-1. Dose reduction was required in 10 patients because of grade 4 neutropenia (five patients), grade 3 fatigue (1 patient), grade 2 fatigue with grade 2 appetite loss (one patient), grade 2 nausea (two patients) and grade 3 rash (1). The reasons for treatment discontinuation in phase II were radiological disease progression (33 patients), clinical disease progression (two patients), recurrent grade 4 neutropenia despite dose reduction due to grade 4 neutropenia (two patients), grade 4 myocardial infarction (one patients) and patient request to return to his distant hometown (one patient). All patients who discontinued treatment because of adverse events recovered from the toxicities after discontinuation. Twelve patients received third-line chemotherapy after discontinuation of FGS: S-1 monotherapy in four patients, gemcitabine + S-1 combination therapy on another treatment schedule in three patients, chemoradiotherapy with S-1 in one patient and new molecularly targeted agents in four patients who participated in a different clinical trial. Twenty-two patients received best supportive care, the other five patients transferred to another hospital, and no

information is available about their treatment after discontinuation of FGS.

## Toxicity

All patients in steps 1 and 2 were evaluated for toxicity. In step 1, grade 3/4 non-hematological toxicity was observed in two patients (grade 3 fatigue during the third course in one patient, grade 3 stomatitis during the second course in one patient). No grade 4 leukocytopenia was observed at any dose level, but grade 4 neutropenia was observed in one out of three patients at dose level 1, none of the three patients at dose level 2, two of the six patients at dose level 3 and all three of the patients at dose level 4. Grade 3 thrombocytopenia was observed in one patient at dose level 2.

Table 4 summarizes the toxicities in the 40 patients who received the RD (level 3). All 40 eligible patients were assessable for toxicities, and FGS combination therapy at the RD was generally well tolerated. The most common toxicities were leukocytopenia (60%) and neutropenia (60%), but most of these toxicities were tolerable and reversible. Grade 4 neutropenia was noted as hematological toxicity in five patients (13%). Grade 3 non-hematological toxicities consisted of fatigue (one patient), vomiting (one patient), rash (one patient) and liver abscess (one patient). The patient who developed the grade 3 liver abscesses recovered after appropriate treatment with intravenous antibiotic alone. One female patient, who had hypercholesterolemia and history of smoking of 30 cigarettes/day, experienced a grade 4 acute myocardial infarction on day 1 of the third course of treatment, after gemcitabine had been administered but before the start of oral S-1. Emergency coronary angiography showed total occlusion of the left anterior descending coronary artery. The patient recovered from the cardiogenic shock due to myocardial infarction after coronary stent implantation and appropriate supportive treatment. S-1 monotherapy for the pancreatic cancer was started about 1 month after the infarction. No other severe or unexpected toxicities were noted in any of the patients.

**Table 4** Treatment-related adverse events among the 40 patients who received the recommended dosages: highest grade reported during the treatment period

| | Grade | | | | Grade 1–4 | Grade 3–4 |
|---|---|---|---|---|---|---|
| | *n* | | | | | |
| | 1 | 2 | 3 | 4 | *n* (%) | *n* (%) |
| Hematological toxicities | | | | | | |
| Leukocytes | 11 | 4 | 9 | 0 | 24 (60) | 9 (23) |
| Neutrophils | 10 | 1 | 8 | 5 | 24 (60) | 13 (33) |
| Hemoglobin | 5 | 11 | 1 | 0 | 17 (43) | 1 (3) |
| Platelets | 11 | 2 | 1 | 0 | 14 (35) | 1 (3) |
| Non-hematological toxicities | | | | | (0) | |
| Aspartate aminotransferase | 8 | 1 | 0 | 0 | 9 (23) | 0 (0) |
| Alanine aminotransferase | 8 | 3 | 0 | 0 | 11 (28) | 0 (0) |
| Alkaline phosphatase | 5 | 2 | 0 | 0 | 7 (18) | 0 (0) |
| Total bilirubin | 3 | 0 | 0 | 0 | 3 (8) | 0 (0) |
| Fatigue | 15 | 2 | 1 | 0 | 18 (45) | 1 (3) |
| Nausea | 13 | 4 | 0 | 0 | 17 (43) | 0 (0) |
| Vomiting | 8 | 1 | 1 | 0 | 10 (25) | 1 (3) |
| Anorexia | 19 | 6 | 0 | 0 | 27 (68) | 0 (0) |
| Stomatitis | 4 | 0 | 0 | 0 | 4 (10) | 0 (0) |
| Alopecia | 8 | 0 | – | – | 8 (20) | – |
| Diarrhea | 7 | 2 | 0 | 0 | 9 (23) | 0 (0) |
| Rash | 3 | 4 | 1 | 0 | 8 (20) | 1 (3) |
| Hyperpigmentation | 9 | 1 | – | – | 10 (25) | – |
| Hand-foot skin reaction | 1 | 2 | 0 | 0 | 3 (8) | 0 (0) |
| Watery eye | 2 | 0 | 0 | – | 2 (5) | 0 (0) |
| Hoarseness | 1 | 0 | 0 | 0 | 1 (3) | 0 (0) |
| Infection liver abscess | 0 | 0 | 1 | 0 | 1 (3) | 1 (3) |
| Myocardial infarction | 0 | 0 | 0 | 1 | 1 (3) | 1 (3) |

Three patients died within 30 days after the final dose of the study drug. All 3 of the deaths were attributed to disease progression, and there were no treatment-related deaths.

### Efficacy

It was possible to assess all 40 eligible patients who received the RD for response. Thirty-four patients had died by the completion of the follow-up period. There were no complete responses, but a partial response was achieved in seven patients (18, 95% confidence interval, 7.3–32.8%). Stable disease was noted in 19 patients (48%) and progressive disease in 14 patients (35%). Tumor responses to second-line FGS therapy are classified according to the tumor responses to first-line gemcitabine in Table 5. Three of 10 patients whose best response was progression disease in first-line chemotherapy achieved partial response in FGS therapy. The median progression-free survival time was 2.8 months. The median overall survival time after the start of second-line therapy was 7.0 months (range 1.3–18.9+), and the 1-year survival rate was 18% (Fig. 1). The median overall survival time after the start of first-line therapy was 13.9 months (range 5.2–31.4).

**Table 5** Objective tumor response

| Response (2nd line) | *n* (%) | Response (1st line) | | |
|---|---|---|---|---|
| | | PR | SD | PD |
| PR | 7 (18) | 1 | 3 | 3 |
| SD | 19 (48) | 3 | 12 | 4 |
| PD | 14 (35) | 2 | 9 | 3 |
| Total | 40 (100) | 6 | 24 | 10 |

Response rate: 18% (95% CI: 7.3–32.8)

RECIST criteria

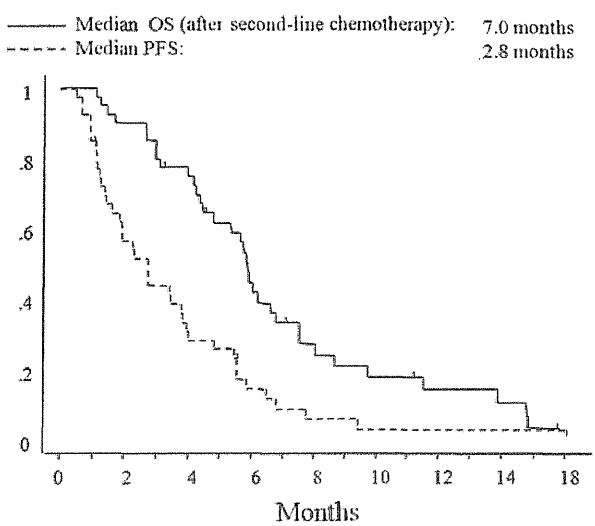


**Fig. 1** Survival curves. Survival ($n = 40$). Progression-free survival (*dashed line*) and overall survival time (*solid line*) curves of patients with gemcitabine-refractory pancreatic cancer receiving systemic chemotherapy with FGS

## Discussion

In the last decade, several clinical trials (mainly phase II) have been conducted in patients with advanced pancreatic cancer after failure of first-line gemcitabine or a gemcitabine-based combination regimen. The results of a randomized trial ($n = 168$) comparing fluorouracil and folinic acid versus oxaliplatin, fluorouracil and folinic acid (OFF) indicated that OFF improved progression-free survival and overall survival as a second-line chemotherapy. The median progression-free survival time and median survival time of OFF were 3 and 6 months, respectively [22]. In the present study, FGS yielded a median progression-free survival time of 2.8 months and a median overall survival time of 7.0 months, similar to the data mentioned above. Furthermore, the response rate of 18% in the present study was above the pre-established boundary (objective response in five or more of the 40 patients) required for the regimen to be considered effective. However, the gap between the median overall survival time and the median progression-free survival time in the present study was relatively large. Although the reason for this gap is unknown, a bias arising from the selection of patients with a good general condition or with a small tumor burden may explain these findings.

Whether gemcitabine as an FDR infusion is active even after progression during treatment with the standard 30-min administration of gemcitabine was the critical clinical question examined in this study. Differentiating between the relative roles of gemcitabine and S-1 in overcoming tumor resistance is difficult. The efficacy and survival data obtained in the present study seem to be better than those of previous studies for oral fluoropyrimidine monotherapy as a salvage chemotherapy for advanced pancreatic carcinoma (Table 6) [1, 2, 17, 28, 29]. However, since all the data were obtained in single-arm studies, a randomized study is needed to make these suggestions reliable. Furthermore, whether the combined regimen in the present study is superior to other regimens, such as the OFF regimen, remains an essential clinical question.

Safety and convenience as well as antitumor efficacy are critically important issues with regard to second-line chemotherapy. One patient experienced an acute myocardial infarction. Although she had other risk factors, such as a smoking habit and hyperlipidemia, a relation between gemcitabine and the acute myocardial infarction cannot be ruled out because gemcitabine had been administered on the day of the infarction. The toxicity profile of FGS

**Table 6** Comparison between the current study and previous studies of oral fluoropyrimidine monotherapy as salvage chemotherapy for advanced pancreatic carcinoma

| Study | References | Phase | Regimen | *n* | PR + CR (%) | Median PFS (months) | Median OS (months) |
|---|---|---|---|---|---|---|---|
| Morizane et al. | [12] | II | S-1 | 40 | 15 | 2.0 | 4.5 |
| Abbruzzese et al. | [29] | II | S-1 | 45 | 0 | 1.4 | 3.1 |
| Sudo et al. | [31] | II | S-1 | 21 | 9.5 | 4.1 | 6.3 |
| Todaka et al. | [32] | Retrospective | S-1 | 52 | 4 | 2.1 | 5.8 |
| Boeck et al. | [30] | II | Capecitabine | 39 | 0 | 2.3 | 7.6 |
| Morizane et al. | Current study | II | FGS | 40 | 18 | 2.8 | 7.0 |

therapy in the other patients was acceptable, and the most common grade 1–4 adverse reactions were anorexia (68%), leukocytopenia (60%) and neutropenia (60%), although most episodes were tolerable and reversible. The safety profile in this study suggests that FGS can be safely administered to pancreatic cancer patients even in a second-line setting, at least in select populations. The biweekly schedule allows enough time to recover from myelosuppression and non-hematological toxicities before the following cycle, enabling patients to receive treatment as scheduled. Actually, the relative dose intensities of gemcitabine and S-1 in our study were high (90.8 and 90.1%, respectively). Furthermore, because of the biweekly schedule, patients do not need to come to the hospital for treatment as often compared with the first-line standard schedule of gemcitabine therapy. Our new treatment schedule may therefore improve the patients' quality of life during anticancer treatment.

We concluded that combination therapy consisting of gemcitabine as a fixed dose rate infusion and S-1 (FGS) provided a promising antitumor activity and tolerable toxicity in patients with gemcitabine-refractory metastatic pancreatic cancer. A larger randomized controlled trial is needed to confirm the clinical benefits of FGS following gemcitabine failure.

## References


1. Abbruzzese JL, Lenz H, Hanna W, Kindler HL, Scullin D, Nemunaitis J, Kudva G, Zhang J, Zergebel C, Urrea P (2009) Open-label phase II study of S-1 as second-line therapy for patients with metastatic pancreatic cancer. 2009 Gastrointestinal Cancers Symposium Abstract No: 243
2. Boeck S, Wilkowski R, Bruns CJ, Issels RD, Schulz C, Moosmann N, Laessig D, Haas M, Golf A, Heinemann V (2007) Oral capecitabine in gemcitabine-pretreated patients with advanced pancreatic cancer. Oncology 73:221–227
3. Bruckner HW, Zhou G, Haenel P, Szraijer L, Greenspan E, Kurbacher CM (1998) Ex vivo ATP tumor testing of gemcitabine for combination chemotherapy and biochemical modulation. Proc Am Assoc Cancer Res 39
4. Conroy T, Desseigne F, Ychou M, Bouche O, Guimbaud R, Becouarn Y, Adenis A, Raoul JL, Gourgou-Bourgade S, de la Fouchardiere C, Bennouna J, Bachet JB, Khemissa-Akouz F, Pere-Verge D, Delbaldo C, Assenat E, Chauffert B, Michel P, Montoto-Grillot C, Ducreux M (2011) FOLFIRINOX versus gemcitabine for metastatic pancreatic cancer. N Engl J Med 364:1817–1825
5. Demols A, Peeters M, Polus M, Marechal R, Gay F, Monsaert E, Hendlisz A, Van Laethem JL (2006) Gemcitabine and oxaliplatin (GEMOX) in gemcitabine refractory advanced pancreatic adenocarcinoma: a phase II study. Br J Cancer 94:481–485
6. Ducreux M, Mitry E, Ould-Kaci M, Boige V, Seitz JF, Bugat R, Breau JL, Bouche O, Etienne PL, Tigaud JM, Morvan F, Cvitkovic E, Rougier P (2004) Randomized phase II study evaluating oxaliplatin alone, oxaliplatin combined with infusional 5-FU, and infusional 5-FU alone in advanced pancreatic carcinoma patients. Ann Oncol 15:467–473
7. Furuse J, Okusaka T, Boku N, Ohkawa S, Sawaki A, Masumoto T, Funakoshi A (2008) S-1 monotherapy as first-line treatment in patients with advanced biliary tract cancer: a multicenter phase II study. Cancer Chemother Pharmacol 62:849–855
8. Green SJ, Benedetti J, Crowley J (1997) Clinical trials in oncology, 2nd edn. Chapman and Hall/CRC, London, pp 53–58
9. Green SJ, Dahlberg S (1992) Planned versus attained design in phase II clinical trials. Stat Med 11:853–862
10. Heinemann V, Xu YZ, Chubb S, Sen A, Hertel LW, Grindey GB, Plunkett W (1990) Inhibition of ribonucleotide reduction in CCRF-CEM cells by 2', 2'-difluorodeoxycytidine. Mol Pharmacol 38:567–572
11. Inuyama Y, Kida A, Tsukuda M, Kohno N, Satake B (2001) Late phase II study of S-1 in patients with advanced head and neck cancer. Gan To Kagaku Ryoho 28:1381–1390
12. Kawahara M, Furuse K, Segawa Y, Yoshimori K, Matsui K, Kudoh S, Hasegawa K, Niitani H (2001) Phase II study of S-1, a novel oral fluorouracil, in advanced non-small-cell lung cancer. Br J Cancer 85:939–943
13. Kim R (2011) FOLFIRINOX: a new standard treatment for advanced pancreatic cancer? Lancet Oncol 12:8–9
14. Koizumi W, Kurihara M, Nakano S, Hasegawa K (2000) Phase II study of S-1, a novel oral derivative of 5-fluorouracil, in advanced gastric cancer. For the S-1 cooperative gastric cancer study group. Oncology 58:191–197
15. Kozuch P, Grossbard ML, Barzdins A, Araneo M, Robin A, Frager D, Homel P, Marino J, DeGregorio P, Bruckner HW (2001) Irinotecan combined with gemcitabine, 5-fluorouracil, leucovorin, and cisplatin (G-FLIP) is an effective and noncross-resistant treatment for chemotherapy refractory metastatic pancreatic cancer. Oncologist 6:488–495
16. Lee GW, Kim HJ, Ju JH, Kim SH, Kim HG, Kim TH, Jeong CY, Kang JH (2009) Phase II trial of S-1 in combination with gemcitabine for chemo-naive patients with locally advanced or

metastatic pancreatic cancer. Cancer Chemother Pharmacol 64:707–713
17. Morizane C, Okusaka T, Furuse J, Ishii H, Ueno H, Ikeda M, Nakachi K, Najima M, Ogura T, Suzuki E (2009) A phase II study of S-1 in gemcitabine-refractory metastatic pancreatic cancer. Cancer Chemother Pharmacol 63:313–319
18. Nakamura K, Yamaguchi T, Ishihara T, Sudo K, Kato H, Saisho H (2006) Phase II trial of oral S-1 combined with gemcitabine in metastatic pancreatic cancer. Br J Cancer 94:1575–1579
19. Oh DY, Cha Y, Choi IS, Yoon SY, Choi IK, Kim JH, Oh SC, Kim CD, Kim JS, Bang YJ, Kim YH (2010) A multicenter phase II study of gemcitabine and S-1 combination chemotherapy in patients with unresectable pancreatic cancer. Cancer Chemother Pharmacol 65:527–536
20. Ohtsu A, Baba H, Sakata Y, Mitachi Y, Horikoshi N, Sugimachi K, Taguchi T (2000) Phase II study of S-1, a novel oral fluorophyrimidine derivative, in patients with metastatic colorectal carcinoma. S-1 cooperative colorectal carcinoma study group. Br J Cancer 83:141–145
21. Okusaka T, Funakoshi A, Furuse J, Boku N, Yamao K, Ohkawa S, Saito H (2008) A late phase II study of S-1 for metastatic pancreatic cancer. Cancer Chemother Pharmacol 61:615–621
22. Pelzer U, Kubica K, Stieler J, Schwaner I, Heil G, Görner M, Mölle M, Hilbig A, Dörken B, Riess H, Oettle H (2008) A randomized trial in patients with gemcitabine refractory pancreatic cancer. Final results of the CONKO 003 study. J Clin Oncol 26(15S) (May 20 Supplement), ASCO Annual Meeting Proceedings (Post-Meeting Edition)
23. Ren Q, Kao V, Grem JL (1998) Cytotoxicity and DNA fragmentation associated with sequential gemcitabine and 5-fluoro-2'-deoxyuridine in HT-29 colon cancer cells. Clin Cancer Res 4:2811–2818
24. Reni M, Cordio S, Milandri C, Passoni P, Bonetto E, Oliani C, Luppi G, Nicoletti R, Galli L, Bordonaro R, Passardi A, Zerbi A, Balzano G, Aldrighetti L, Staudacher C, Villa E, Di Carlo V (2005) Gemcitabine versus cisplatin, epirubicin, fluorouracil, and gemcitabine in advanced pancreatic cancer: a randomised controlled multicentre phase III trial. Lancet Oncol 6:369–376
25. Saek T, Takashima S, Sano M, Horikoshi N, Miura S, Shimizu S, Morimoto K, Kimura M, Aoyama H, Ota J, Noguchi S, Taguchi T (2004) A phase II study of S-1 in patients with metastatic breast cancer–a Japanese trial by the S-1 cooperative study group, breast cancer working group. Breast Cancer 11:194–202
26. Sakata Y, Ohtsu A, Horikoshi N, Sugimachi K, Mitachi Y, Taguchi T (1998) Late phase II study of novel oral fluoropyrimidine anticancer drug S-1 (1 M tegafur-0.4 M gimestat-1 M otastat potassium) in advanced gastric cancer patients. Eur J Cancer 34:1715–1720
27. Shirasaka T, Shimamato Y, Ohshimo H, Yamaguchi M, Kato T, Yonekura K, Fukushima M (1996) Development of a novel form of an oral 5-fluorouracil derivative (S-1) directed to the potentiation of the tumor selective cytotoxicity of 5-fluorouracil by two biochemical modulators. Anticancer Drugs 7:548–557
28. Sudo K, Yamaguchi T, Nakamura K, Denda T, Hara T, Ishihara T, Yokosuka O (2011) Phase II study of S-1 in patients with gemcitabine-resistant advanced pancreatic cancer. Cancer Chemother Pharmacol 67:249–254
29. Todaka A, Fukutomi A, Boku N, Onozawa Y, Hironaka S, Yasui H, Yamazaki K, Taku K, Machida N, Sakamoto T, Tomita H (2010) S-1 monotherapy as second-line treatment for advanced pancreatic cancer after gemcitabine failure. Jpn J Clin Oncol 40:567–572
30. Tsavaris N, Kosmas C, Skopelitis H, Gouveris P, Kopterides P, Loukeris D, Sigala F, Zorbala-Sypsa A, Felekouras E, Papalambros E (2005) Second-line treatment with oxaliplatin, leucovorin and 5-fluorouracil in gemcitabine-pretreated advanced pancreatic cancer: a phase II study. Invest New Drugs 23:369–375
31. Ueno H, Okusaka T, Furuse J, Yamao K, Funakoshi A, Boku N, Ohkawa S, Yokosuka O, Tanaka K, Moriyasu F, Nakamori S, Sato T (2011) Multicenter phase II study of gemcitabine and S-1 combination therapy (GS Therapy) in patients with metastatic pancreatic cancer. Jpn J Clin Oncol 41:953–958
32. Ueno H, Okusaka T, Ikeda M, Takezako Y, Morizane C (2004) Phase II study of S-1 in patients with advanced biliary tract cancer. Br J Cancer 91:1769–1774
33. Ueno H, Okusaka T, Ikeda M, Takezako Y, Morizane C (2005) An early phase II study of S-1 in patients with metastatic pancreatic cancer. Oncology 68:171–178
34. Ulrich-Pur H, Raderer M, Verena Kornek G, Schull B, Schmid K, Haider K, Kwasny W, Depisch D, Schneeweiss B, Lang F, Scheithauer W (2003) Irinotecan plus raltitrexed vs raltitrexed alone in patients with gemcitabine-pretreated advanced pancreatic adenocarcinoma. Br J Cancer 88:1180–1184